Arf1 orchestrates Rab GTPase conversion at the *trans*-Golgi network

Laura L. Thomas†, Carolyn M. Highland, and J. Christopher Fromme*
Department of Molecular Biology and Genetics, Weill Institute for Cell and Molecular Biology, Cornell University, Ithaca, NY 14853

ABSTRACT **Rab family GTPases are key organizers of membrane trafficking and function as markers of organelle identity. Accordingly, Rab GTPases often occupy specific membrane domains, and mechanisms exist to prevent the inappropriate mixing of distinct Rab domains. The yeast Golgi complex can be divided into two broad Rab domains: Ypt1 (Rab1) and Ypt6 (Rab6) are present at the early/medial Golgi and sharply transition to Ypt31/32 (Rab11) at the late Golgi/*trans*-Golgi network (TGN). This Rab conversion has been attributed to GTPase-activating protein (GAP) cascades in which Ypt31/32 recruits the Rab-GAPs Gyp1 and Gyp6 to inactivate Ypt1 and Ypt6, respectively. Here we report that Rab transition at the TGN involves additional layers of regulation. We provide new evidence confirming the TRAPPII complex as an important regulator of Ypt6 inactivation and uncover an unexpected role of the Arf1 GTPase in recruiting Gyp1 to drive Ypt1 inactivation at the TGN. Given its established role in directly recruiting TRAPPII to the TGN, Arf1 is therefore a master regulator of Rab conversion on maturing Golgi compartments.**

Monitoring Editor
Benjamin Glick
University of Chicago

Received: Oct 27, 2020
Revised: Mar 16, 2021
Accepted: Mar 19, 2021

INTRODUCTION

The Golgi complex functions as the major sorting center of eukaryotic cells, coordinating cargo traffic in both the biosynthetic and endocytic recycling pathways. Golgi transport is orchestrated by Arf and Rab family GTPases, which recruit diverse effectors that mediate vesicle formation, transport, tethering, and fusion (Stenmark, 2009; Donaldson and Jackson, 2011). GTPase activity is controlled by the opposing action of specific guanine nucleotide exchange factors (GEFs) and GTPase-activating proteins (GAPs) (Barr and Lambright, 2010; Müller and Goody, 2018). GEFs activate Arf and Rab substrates by catalyzing guanosine triphosphate (GTP)/guanosine diphosphate (GDP) exchange, and active GTP-bound GTPases are stabilized on target membranes. GAPs catalyze the reverse process by driving GTP hydrolysis to inactivate substrates, and inactive GDP-bound GTPases are rendered cytosolic. Therefore, GEFs and GAPs play a key role not only in regulating Arf and Rab activity, but also localization. Rab family GTPases largely function in mediating the tethering of vesicles with acceptor compartments and are thus proposed to serve as markers of organelle identity (Zerial and McBride, 2001; Pfeffer, 2013). As such, Rab GTPases often occupy distinct "Rab domains" on organelle membranes, and exclusion of other Rabs from these domains is critical in maintaining fidelity of membrane transport.

In the budding yeast model system, three Rab GTPases coordinate membrane traffic at the Golgi complex. Ypt1 (Rab1) mediates fusion of endoplasmic reticulum (ER)-derived COPII vesicles with the early Golgi and also regulates several transport events at the medial/late Golgi (Jedd *et al.*, 1995; Sclafani *et al.*, 2010). Ypt6 (Rab6) facilitates endosome-to-Golgi transport by capturing incoming vesicles at the medial/late Golgi (Kawamura *et al.*, 2014). Ypt31/32 (Rab11) is activated at the *trans*-Golgi network (TGN) where it mediates secretory vesicle biogenesis and subsequent transport to the plasma membrane (PM) (Jedd *et al.*, 1997). An additional major regulator of Golgi transport is the GTPase Arf1, which recruits a multitude of effectors to drive vesicle formation throughout the Golgi complex (Cherfils, 2014). The specific GEFs that activate Ypt1, Ypt6, and Ypt31/32 are the TRAPPIII, Ric1/Rgp1, and

This article was published online ahead of print in MBoC in Press (http://www.molbiolcell.org/cgi/doi/10.1091/mbc.E20-10-0664) on March 31, 2021.

Conflict of interest: The authors declare no competing interests.

Author contributions: Conceptualization, methodology, and writing, L.L.T., C.M.H., and J.C.F.; investigation and formal analysis, L.L.T. and C.M.H.

†Present address: HHMI and Department of Molecular Biology and Genetics, Johns Hopkins University School of Medicine, Baltimore, MD 21205.

*Address correspondence to: J. Christopher Fromme (jcf14@cornell.edu).

Abbreviations used: GAP, GTPase-activating protein; GEF, guanine nucleotide exchange factor; PC, phosphatidylcholine; PM, plasma membrane; TGN, *trans*-Golgi network.

TRAPPII complexes, respectively (Siniossoglou *et al.*, 2000; Pusapati *et al.*, 2012; Thomas *et al.*, 2019), whereas Arf1 is activated by Gea1/2 at the early/medial Golgi and Sec7 at the late Golgi/TGN (Peyroche *et al.*, 1996; Spang *et al.*, 2001; Casanova, 2007). Of note to this study, Arf1 plays an important role in Ypt31/32 activation by recruiting TRAPPII to the TGN (Thomas and Fromme, 2016). Although several Rab-GAPs have been shown to act on multiple substrates in vitro (Du *et al.*, 1998; Albert and Gallwitz, 1999), the biologically relevant GAPs that coordinate Ypt1 and Ypt6 inactivation at the Golgi are Gyp1 and Gyp6, respectively (Strom *et al.*, 1993; Du and Novick, 2001; Will and Gallwitz, 2001).

Previous studies have found that both Ypt1 and Ypt6 display very little overlap with Ypt31/32 at the Golgi (Rivera-Molina and Novick, 2009; Suda *et al.*, 2013; Kim *et al.*, 2016). These live cell imaging experiments have revealed that there is a transition from Ypt1 and Ypt6 to Ypt31/32 on maturing Golgi compartments, indicating that mechanisms exist to precisely terminate Ypt1 and Ypt6 activity as Ypt31/32 accumulates. The exclusion of Ypt1 and Ypt6 from the TGN was subsequently explained by the existence of GAP cascades in which Ypt31/32 recruits both Gyp1 and Gyp6 to drive inactivation of the earlier-acting Rabs (Rivera-Molina and Novick, 2009; Suda *et al.*, 2013). Since these initial studies, countercurrent GAP cascades have emerged as a common mechanism for regulating the directionality of membrane transport pathways and limiting overlap of distinct Rab domains (Pfeffer, 2012; Novick, 2016). However, a recent study raised the possibility that additional factors may influence Rab transition at the TGN: the TRAPPII complex was found to interact with Gyp6 to drive Ypt6 inactivation (Brunet *et al.*, 2016). Furthermore, levels of both Ypt1 and Ypt6 decline at the late Golgi before robust Ypt31/32 activation, suggesting that Gyp1 and Gyp6 recruitment may be initiated by factors other than Ypt31/32.

Here we investigate the regulatory mechanisms that control Rab conversion on maturing Golgi compartments. In agreement with Brunet *et al.* (2016), we present additional evidence demonstrating that the TRAPPII complex is an important recruiter of Gyp6 and that TRAPPII is required for robust Ypt6 inactivation at the TGN. We also discover an unexpected role of Arf1 in directly recruiting Gyp1 to drive Ypt1 inactivation. Arf1 is an established mediator of TRAPPII recruitment; therefore Arf1 is a master regulator of Rab transition at the TGN.

RESULTS

Gyp6 and Gyp1 are recruited to the Golgi before peak Ypt31/32 activation

We began by examining the localization of endogenous, mNeonGreen-tagged Gyp6 and Gyp1 relative to established early and late Golgi markers. In agreement with previous studies, Gyp6 was highly enriched at Sec7-labeled late Golgi/TGN compartments but did not colocalize with the early Golgi marker Gea1 (Figure 1A) (Suda *et al.*, 2013; Kawamura *et al.*, 2014). Gyp6 also displayed extensive overlap with TRAPPII, supporting a model in which TRAPPII facilitates Gyp6 recruitment to the Golgi (Brunet *et al.*, 2016). Moreover, the Gyp6 substrate Ypt6 showed minimal overlap with TRAPPII (Supplemental Figure S1A), further supporting a role for TRAPPII in mediating Ypt6 inactivation. In contrast to Gyp6, Gyp1 displayed modest colocalization with both early and late Golgi/TGN markers (Figure 1B), indicating that Gyp1 is broadly present across Golgi compartments. We also found that the Rab-GAP Gyp2, which inactivates Ypt31/32 in the late secretory pathway (Lafourcade *et al.*, 2003; Sciorra *et al.*, 2005), localized to punctate structures that did not overlap with Gea1 and showed minimal colocalization with Sec7 (Supplemental Figure S1B).

We next used time-lapse imaging to observe GAP dynamics at the late Golgi/TGN. We previously determined that Gyp1 accumulates progressively at Golgi compartments, with Gyp1 recruitment peaking directly downstream of Sec7 recruitment (Thomas *et al.*, 2018). We found that Gyp6 began to accumulate after Sec7, but both proteins peaked in intensity at approximately the same time (Figure 1C), consistent with an enrichment of Gyp6 at the late Golgi. We previously observed that TRAPPII displays very similar dynamics (Thomas and Fromme, 2016), again in agreement with a model in which TRAPPII recruits Gyp6 to the Golgi.

Previous studies have elucidated countercurrent GAP cascades in which the downstream Rab Ypt31/32 recruits Gyp6 and Gyp1 to inactivate the upstream Rabs Ypt6 and Ypt1, respectively (Rivera-Molina and Novick, 2009; Suda *et al.*, 2013). However, Ypt31/32 is activated relatively late at the TGN, with peak Ypt31/32 activation occurring 10–20 s after Sec7 peak recruitment (Figure 1C; McDonold and Fromme, 2014; Thomas and Fromme, 2016). We found that Gyp1 is present at early Golgi compartments and that Gyp6 levels at the late Golgi peak before peak Ypt31/32 activation (Figure 1D). This suggests that recruitment of Gyp6 and Gyp1 to the Golgi is mediated by factors in addition to Ypt31/32.

TRAPPII is required for Gyp6 localization, and Arf1 is required for Gyp1 localization

Our observation that Gyp1 is present at the early Golgi as well as analysis of Gyp6 and Gyp1 dynamics suggest that Ypt31/32 is not responsible for the initial recruitment of these Rab-GAPs. We therefore sought to identify additional factors controlling Gyp6 and Gyp1 localization. As both GAPs accumulate at the late Golgi directly downstream of Sec7, we began by testing whether Arf1 activation is required for their localization. We treated cells with MNTC, which significantly reduces the activation of Arf1 (Supplemental Figure S2A). We have previously determined that MNTC treatment causes TRAPPII mislocalization and a consequent reduction in Ypt31/32 activation (Supplemental Figure S2, B and C) (Thomas and Fromme, 2016). Therefore, MNTC impairs Golgi localization of Arf1, TRAPPII, and Ypt31/32.

We found that MNTC treatment mislocalized Gyp6 to the cytosol (Figure 2A and Supplemental Figure S2B), indicating that Arf1 activation is required for Gyp6 recruitment to the Golgi. MNTC treatment also mislocalized Gyp1 to the cytosol, though several small Gyp1 puncta often remained that did not colocalize with Sec7 (Figure 2B and Supplemental Figure S2C). We considered that these puncta might represent Gyp1 present at the early Golgi; however, they showed minimal overlap with the early Golgi marker Gea1 (Supplemental Figure S2D). In contrast to Gyp6 and Gyp1, MNTC treatment did not result in cytoplasmic localization of the Ypt31/32 GAP Gyp2. Instead Gyp2 became heavily enriched at late Golgi/TGN compartments following treatment with MNTC (Supplemental Figure S2E), indicating that MNTC does not disrupt membrane association of all factors downstream of Sec7.

As MNTC affects multiple Golgi regulators, we next examined Gyp6 and Gyp1 localization in TRAPPII and Arf1 mutants. We used *trs130Δ33* and *trs65Δ* TRAPPII mutants, which cause TRAPPII mislocalization and, consequently, impaired Ypt31/32 activation (Supplemental Figure S3A) (Morozova *et al.*, 2006; Liang *et al.*, 2007; Thomas and Fromme, 2016). Notably, as TRAPPII is an Arf1 effector, TRAPPII mislocalization in either mutant can be partially rescued by Arf1 overexpression (Supplemental Figure S3A) (Thomas and Fromme, 2016). *arf1Δ* mutants are viable due to expression of Arf2, a functionally redundant paralogue that accounts for approximately 10% of total Arf1/2 protein (Stearns *et al.*, 1990). Therefore,

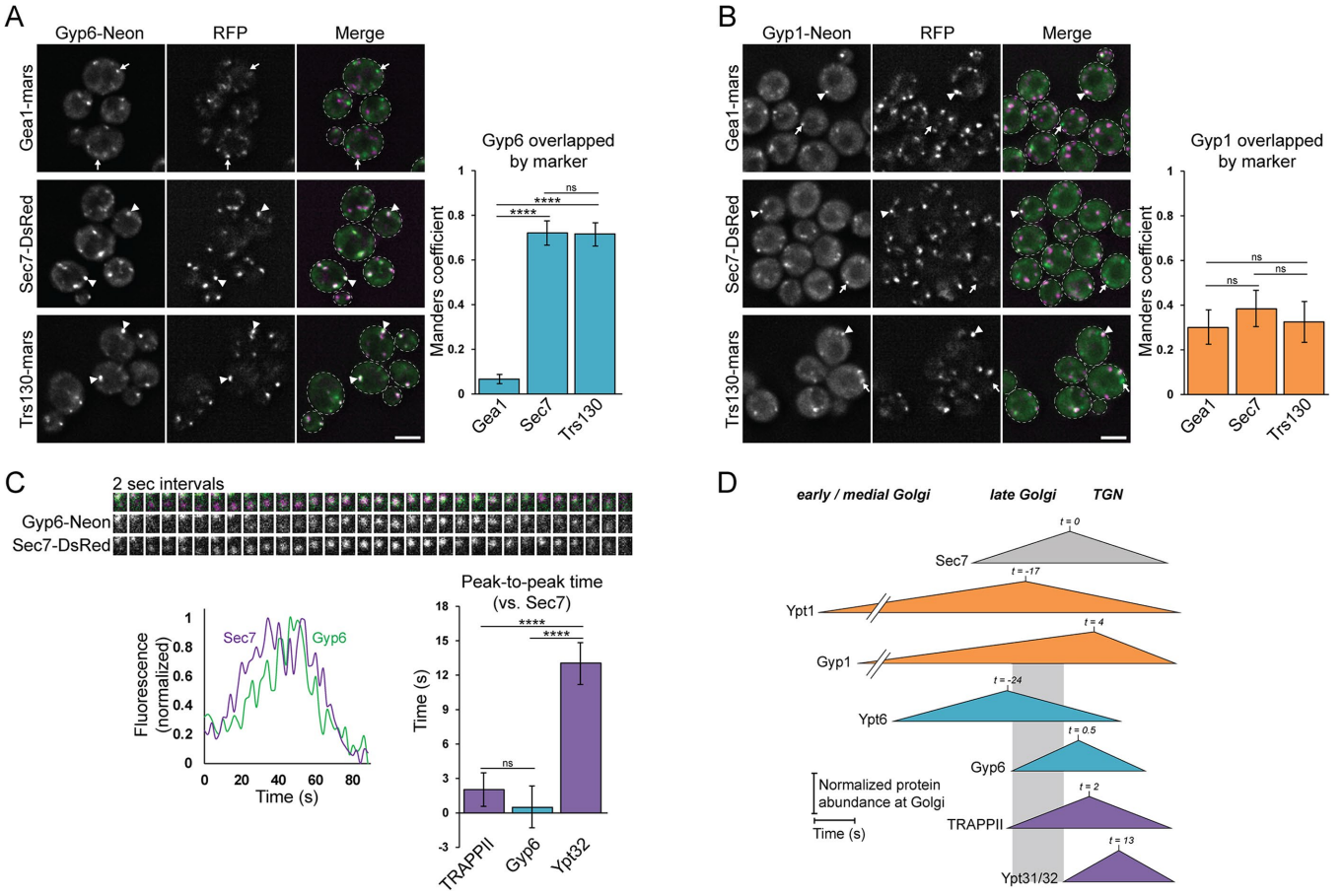

FIGURE 1: Gyp6 and Gyp1 are recruited to Golgi compartments before peak Ypt31/32 activation. (A) Left: Representative images showing Gyp6 localization relative to the early Golgi marker Gea1 or the late Golgi/TGN markers Sec7 and Trs130 (TRAPPII). Right: Quantification of Gyp6 colocalization with each indicated marker measured using the Manders overlap coefficient. Error bars represent 95% CI for $n > 30$ cells. (B) Left: Representative images showing Gyp1 localization relative to Gea1, Sec7, or Trs130. Right: Quantification of Gyp1 colocalization with each indicated marker. Error bars represent 95% CI for $n > 25$ cells. (C) Top: Time-lapse imaging series (2-s intervals) of a single Golgi compartment in cells expressing Gyp6-mNeonGreen and Sec7-6xDsRed. Bottom left: Normalized quantification of Gyp6-mNeonGreen and Sec7-6xDsRed signal from a single Golgi compartment. Bottom right: Quantification of peak-to-peak times for each indicated protein versus Sec7. Error bars represent 95% CI for $n \geq 12$ time-lapse series. Values for TRAPPII and Ypt32 are reproduced from Thomas and Fromme (2016) and Thomas *et al.* (2019). (D) Schematic depicting the dynamics of Rabs, GEFs, and GAPs at a maturing Golgi compartment. *t = 0* is set to peak Sec7 recruitment. Note that Gyp1 is present at early Golgi compartments and that Gyp6 accumulates at the late Golgi with the same dynamics as TRAPPII and before peak Ypt31/32 activation (gray box). Scale bars, 2 μm. White arrowheads and arrows denote colocalization or a lack of colocalization of tagged proteins at Golgi compartments, respectively. n.s., not significant; ****, $P < 0.0001$.

the *arf1*Δ mutation effectively reduces total levels of Arf at the Golgi.

We found that Gyp6 was moderately mislocalized from the late Golgi in the *arf1*Δ mutant and that localization was rescued by plasmid-borne *ARF1* (Figure 2C and Supplemental Figure S3B). Gyp6 was highly mislocalized in both TRAPPII mutants and could not be rescued by an extra copy of *ARF1*. This suggests that TRAPPII is important for Gyp6 localization but that Arf1 does not play a major role in direct Gyp6 recruitment in vivo. Partial mislocalization of Gyp6 in the *arf1*Δ mutant may be due to impaired localization of TRAPPII to the Golgi in *arf1*Δ cells (Thomas and Fromme, 2016).

In contrast to Gyp6, Gyp1 appeared to be completely cytosolic in *arf1*Δ cells but was unaffected by either TRAPPII mutation (Figure 2D). This indicates that wild-type levels of TRAPPII and active Ypt31/32 are not required for robust Gyp1 recruitment. Intriguingly, expression of an extra copy of *ARF1* not only rescued Gyp1 localization in the *arf1*Δ mutant but also enhanced Gyp1 colocalization with Sec7 in wild-type cells (Figure 2, D and E). This suggested to us that that Arf1 might directly recruit Gyp1 to membranes. To further test this hypothesis, we employed the "anchor-away" system (Haruki *et al.*, 2008) to conditionally recruit GTP-locked Arf1(Q71L) to the PM. We found that ectopically localized Arf1(Q71L) recruited Gyp1 to the PM (Figure 2F), further supporting a model in which Arf1 directly mediates Gyp1 membrane association.

We also tested whether Gyp6 or Gyp1 contributes to TRAPPII or Sec7 recruitment but found both GEFs to be localized normally in *gyp6*Δ and *gyp1*Δ mutants (Supplemental Figure S3C). Together, these results suggest that TRAPPII and/or Ypt31/32 are critical for Gyp6 localization and that Arf1 mediates Gyp1 membrane recruitment.

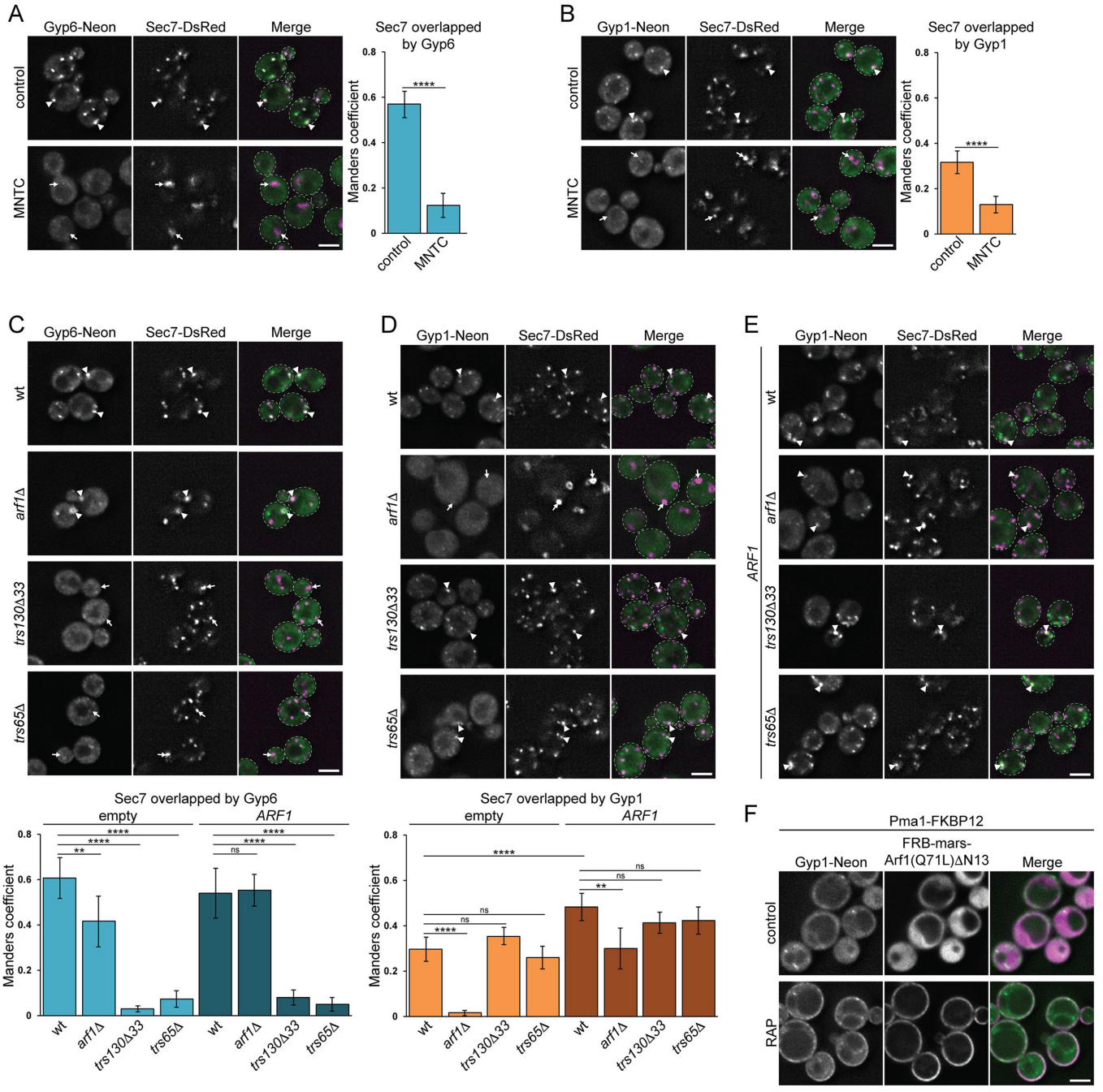

FIGURE 2: TRAPPII and Arf1 are required for Gyp6 and Gyp1 recruitment to the Golgi, respectively. (A) Left: Representative images showing Gyp6 recruitment to Sec7-labeled late Golgi/TGN compartments in untreated cells versus cells treated with the Sec7 inhibitor MNTC (20 μM, 15 min). Right: Quantification of Gyp6 recruitment to the late Golgi/TGN measured using the Manders overlap coefficient. Error bars represent 95% CI for $n > 25$ cells. (B) Left: Representative images showing Gyp1 recruitment to Sec7-labeled late Golgi/TGN compartments in untreated versus MNTC-treated cells (20 μM, 15 min). Right: Quantification of Gyp1 recruitment to the late Golgi/TGN. Error bars represent 95% CI for $n > 25$ cells. (C) Top: Representative images showing Gyp6 recruitment to the late Golgi/TGN in wild-type versus *arf1Δ*, *trs65Δ*, or *trs130Δ33* mutants. Bottom: Quantification of Gyp6 localization to the late Golgi/TGN in each indicated mutant with or without rescue by plasmid-borne *ARF1*. See Supplemental Figure S3B for representative images of Gyp6 localization with Arf1 rescue. Error bars represent 95% CI for $n > 20$ cells. (D) Top: Representative images showing Gyp1 recruitment to the late Golgi/TGN in wild-type versus *arf1Δ*, *trs65Δ*, or *trs130Δ33* mutants. Bottom: Quantification of Gyp1 localization to the late Golgi/TGN in each indicated mutant with or without rescue by plasmid-borne *ARF1*. Error bars represent 95% CI for $n > 25$ cells. (E) Representative images showing Gyp1 localization in wild-type versus *arf1Δ*, *trs65Δ*, or *trs130Δ33* mutants following rescue by plasmid-borne *ARF1*. See panel D for quantification. (F) Representative images of Gyp1 in control cells versus cells with GTP-locked Arf1 (missing most of its N-terminal amphipathic helix) relocalized to the PM via rapamycin (RAP)-induced association with Pma1-FKBP12. Scale bars, 2 μm. White arrowheads and arrows denote colocalization or a lack of colocalization of tagged proteins at Golgi compartments, respectively. n.s., not significant; **, $P < 0.01$; ****, $P < 0.0001$.

TRAPPII binds directly to Gyp6 and Arf1 binds directly to Gyp1 on membranes in vitro

We next tested whether TRAPPII and Arf1 can directly bind to Gyp6 and Gyp1 on synthetic liposome membranes. We purified endogenous Gyp6, Gyp1, and TRAPPII from yeast as well as myristoylated Arf1 from *Escherichia coli* (Figure 3A). As both Rab-GAPs have been previously characterized as Ypt31/32 effectors (Rivera-Molina and Novick, 2009; Suda *et al.*, 2013), we also generated recombinant prenylated Ypt32 in order to directly compare recruitment by Arf1, TRAPPII, and Ypt32. As Gyp6 and Gyp1 recruitment peaks at the TGN (see Figure 1), we performed membrane-binding assays using liposomes with a TGN-like lipid composition (Klemm *et al.*, 2009) and activated all GTPases by inducing them to bind the nonhydrolyzable GTP analogue GMP-PNP. In initial experiments, we found that Gyp6 was strongly recruited by both Arf1 and Ypt32, while Gyp1 was recruited by Arf1 but only weakly recruited by Ypt32 (Supplemental Figure S4A). We observed that both GAPs bound TGN liposomes in the absence of any recruiter but that this binding could be reduced by the addition of 0.04% CHAPS detergent. Therefore, to enhance the stringency of our membrane-binding assays, we included 0.04% CHAPS in all subsequent experiments.

Using this more stringent membrane-binding assay, we compared GAP recruitment by Arf1, Ypt32, and TRAPPII (Figure 3B). We used Arf1 in all reactions containing TRAPPII to facilitate TRAPPII membrane association (Thomas and Fromme, 2016). We found that Gyp6 bound liposomes containing Arf1 alone and that the addition of TRAPPII significantly enhanced Gyp6 membrane association (Figure 3C). Gyp1 was also recruited to membranes by Arf1 alone (Figure 3D), and the addition of TRAPPII reduced Gyp1 membrane association, likely by competing with Gyp1 for binding to Arf1. These in vitro binding results corresponded well with our in vivo results, indicating a role for TRAPPII in recruiting Gyp6, a role for Arf1 in recruiting Gyp1, and a more minor role for Arf1 in recruiting Gyp6.

Under these more stringent conditions, Ypt32 did not recruit either GAP to membranes (Figure 3, C and D). Therefore, we tested whether Ypt32 was able to recruit Sec7, an established Ypt31/32 effector (McDonold and Fromme, 2014; Halaby and Fromme, 2018), under the same conditions. Using the more stringent membrane-binding assay, Ypt32 robustly recruited Sec7 to membranes (Figure 3E), indicating that Ypt32 is functional in effector recruitment under our assay conditions. We also found that Arf1 weakly recruited Sec7 under these conditions, consistent with previous findings that Arf1 recruits Sec7 in a positive-feedback loop (Richardson *et al.*, 2012) but indicating the Sec7 interaction with Ypt32 is stronger. In contrast, Gyp1 is strongly recruited by Arf1 but comparatively weakly recruited by Ypt32 (Figure 3D and Supplemental Figure S4A).

To test for specificity in the membrane-binding assays, we examined whether TRAPPII or Arf1 could recruit other GAP proteins. TRAPPII and Arf1 did not enhance the membrane association of either the Rab-GAP Gyp2 or the Arf-GAP Gcs1 (Supplemental Figure S4, B and C), indicating that Gyp6 and Gyp1 recruitment by TRAPPII and Arf1 is specific. The lack of recruitment of Gcs1 by its substrate Arf1 may be explained by reports that Gcs1 uses its ALPS motif to bind highly curved membranes with lipid-packing defects (Bigay *et al.*, 2003; Xu *et al.*, 2013) and our use of relatively low-curvature 100 nm liposomes in the binding assays. We next used the Arf-like GTPase Arl1 to examine the specificity of Arf1-mediated GAP recruitment. We found that Gyp6 was recruited equally by Arf1 and Arl1, suggesting that despite being strong, the interaction between Gyp6 and Arf1 is not specific (Supplemental Figure S4D). In contrast, Gyp1 was not recruited by Arl1, indicating that the Gyp1-Arf1 interaction is specific. Although we observed that Arf1 recruited Gyp6 more robustly than Gyp1, this is likely due to the apparently higher affinity of Gyp6 for membranes, evidenced by its ability to bind the TGN-like liposomes in the absence of recruiter even under the stringent conditions (Supplemental Figure S4D).

Finally, we tested whether lipid composition is important for Gyp6 and Gyp1 membrane association. Arf1 recruited both GAPs to anionic TGN-like liposomes but was unable to recruit either GAP to neutral phosphatidylcholine (PC) liposomes (Supplemental Figure S4E). The lack of binding to PC membranes is consistent with our observation that both GAPs possess intrinsic affinity for TGN liposomes (Supplemental Figure S4A) and suggests that GAP localization may be mediated in part by membrane composition.

Taken together, we interpret the in vitro and in vivo results to indicate that TRAPPII is important for directly recruiting Gyp6 to the TGN and activated Arf1 is important for directly recruiting Gyp1 to the TGN.

Arf1 and TRAPPII are important for Gyp1 and Gyp6 localization in vivo

We next extended our mutant analysis to test the contribution of Ypt31/32 to GAP localization in vivo. As a control, we first confirmed that Ypt31/32 is required to localize the Rab-GEF Sec2, an established Ypt31/32 effector in both yeast and mammalian cells (Ortiz *et al.*, 2002; Knödler *et al.*, 2010). We examined Sec2 localization in a *ypt32*Δ *ypt31-101* mutant, which is inviable at 38°C (Supplemental Figure S5A). Even at a semipermissive temperature of 30°C, Sec2 was severely mislocalized in the *ypt32*Δ *ypt31-101* mutant (Figure 4A), confirming that Ypt31/32 function is critical for Sec2 membrane recruitment.

In contrast to Sec2, Gyp6 and Gyp1 localization to the Golgi appeared to be largely unaffected in *ypt32*Δ *ypt31-101* cells grown at 30°C (Figure 4, B and C). Furthermore, after shifting to a restrictive temperature of 38°C, the localization of Gyp1 and Gyp6 to puncta was only slightly perturbed. A previous study found that Gyp1 puncta were reduced in the more severe *ypt31*Δ *ypt32*A141D mutant, although Gyp1 expression was also reduced (Rivera-Molina and Novick, 2009). To replicate this experiment, we examined Gyp1 localization in the *ypt31*Δ *ypt32*A141D mutant, which is inviable at temperatures greater than 35°C (Supplemental Figure S5B). We found that Gyp1 membrane association was only marginally impaired in *ypt31*Δ *ypt32*A141D cells grown at 38°C (Figure 4D) and the observed phenotype was less severe than that observed in *arf1*Δ mutant cells (Figure 2D). The more severe Gyp1 and Gyp6 mislocalization phenotypes previously reported in Ypt31/32 mutants may have been due to GAP overexpression from the strong *ADH1* promoter (Rivera-Molina and Novick, 2009; Suda *et al.*, 2013), whereas in the present study GAP expression was driven by endogenous promoters.

To further examine the role of Ypt31/32 in Gyp1 and Gyp6 localization, we next asked whether Ypt31/32 overexpression could rescue GAP mislocalization caused by MNTC inhibition of Golgi Arf activation. As a positive control, we first tested whether Ypt31 overexpression restores recruitment of Sec2, which becomes mislocalized to the cytosol following MNTC treatment. Overexpression of both wild-type Ypt31 and constitutively active GTP-locked Ypt31(Q72L) restored Sec2 localization in cells treated with MNTC (Figure 5A). Furthermore, Ypt31(Q72L) altered Sec2 localization in untreated cells, causing the accumulation of small Sec2 puncta at the cell periphery, presumably corresponding to secretory vesicles. Taking the results together, this

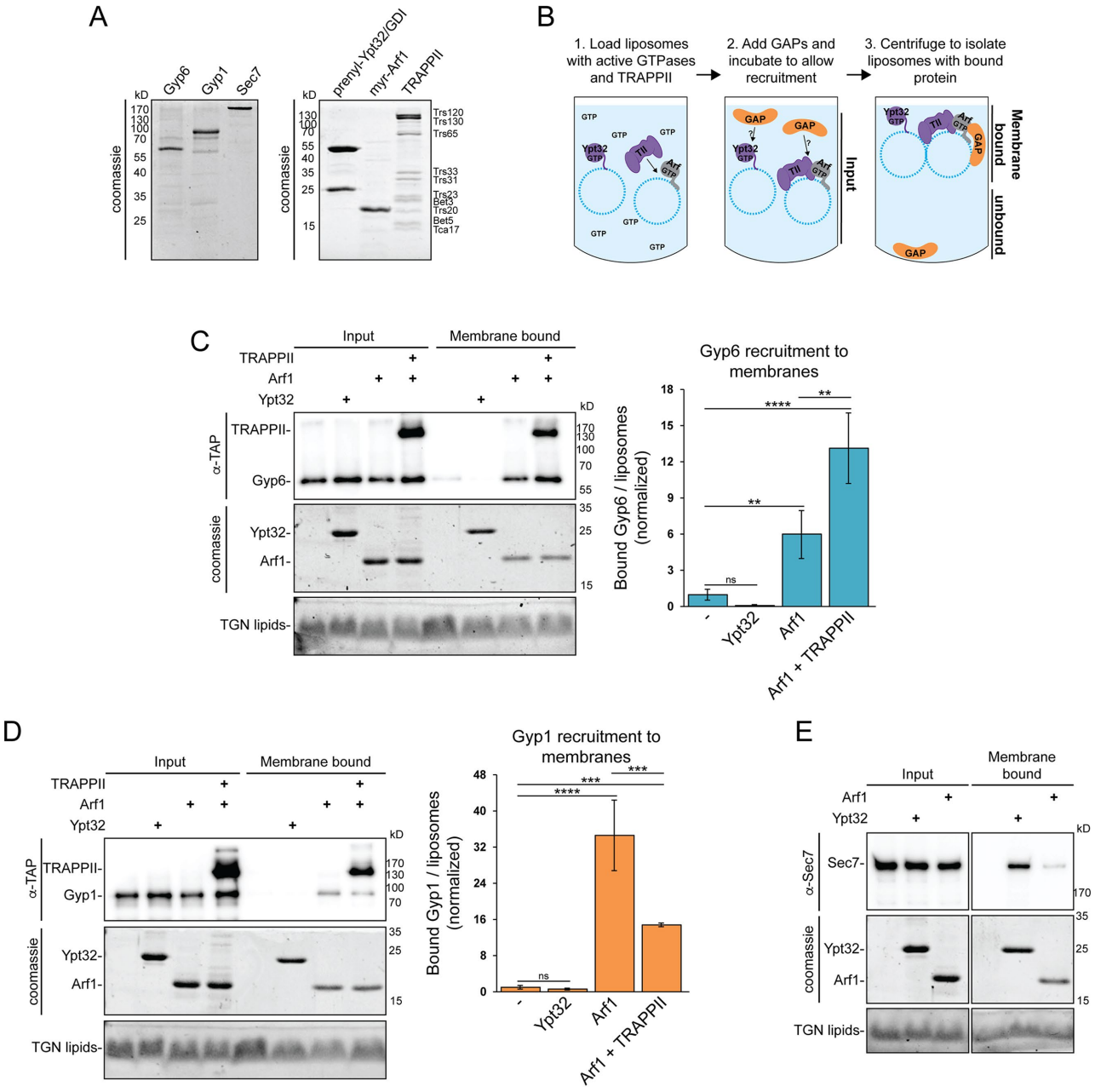

FIGURE 3: TRAPPII and Arf1 recruit Gyp6 and Gyp1 to membranes, respectively. (A) Left: Endogenous Gyp6, Gyp1, and Sec7 were purified from yeast using a TAP tag. Right: Proteins and protein complexes used to test GAP recruitment to membranes. Ypt32 was purified from *E. coli* and subjected to in vitro prenylation, myristoylated Arf1 was purified from *E. coli*, and endogenous TRAPPII was purified from yeast via Trs130-TAP. (B) Schematic depicting liposome flotation assays used to test recruitment of GAPs to membranes: 1) Prenylated Ypt32 or myristoylated Arf1 was activated on liposomes by EDTA-mediated exchange with excess GMP-PNP, a nonhydrolyzable GTP analogue (in this schematic "GTP" denotes GMP-PNP). In some reactions, activated Arf1 was used to recruit TRAPPII (TII) to membranes (Thomas and Fromme, 2016). 2) Purified GAPs were added, and the reactions were incubated to allow for any membrane recruitment. 3) Liposomes and bound protein were separated from unbound protein via centrifugation in a sucrose gradient. (C) Left: Liposome flotation assay testing recruitment of Gyp6 to TGN-like membranes by activated Ypt32, activated Arf1, or a combination of Arf1 and TRAPPII (Arf1 is required for efficient TRAPPII recruitment to membranes). TRAPPII and Gyp6 are visualized by Western blot. Right: Quantification of Gyp6 recruitment to membranes from the flotation reactions at left. Error bars represent 95% CI for $n \geq 3$ replicate reactions. (D) Left: Liposome flotation assay testing recruitment of Gyp1 to TGN membranes by activated Ypt32, activated Arf1, or a combination of Arf1 and TRAPPII. TRAPPII and Gyp1 are visualized by Western blot. Right: Quantification of Gyp1 recruitment to membranes from the flotation reactions at left. Error bars represent 95% CI for $n \geq 3$ replicate reactions. (E) Control liposome flotation assay testing recruitment of Sec7 to TGN membranes by activated Ypt32 or Arf1. Sec7 is a previously characterized effector of both Ypt32 and Arf1 (Richardson *et al.*, 2012; McDonold and Fromme, 2014). Sec7 is visualized by Western blot. Reaction conditions are identical to those used to test Gyp6 and Gyp1 recruitment in panels C and D. n.s., not significant; **, $P < 0.01$; ***, $P < 0.001$; ****, $P < 0.0001$.

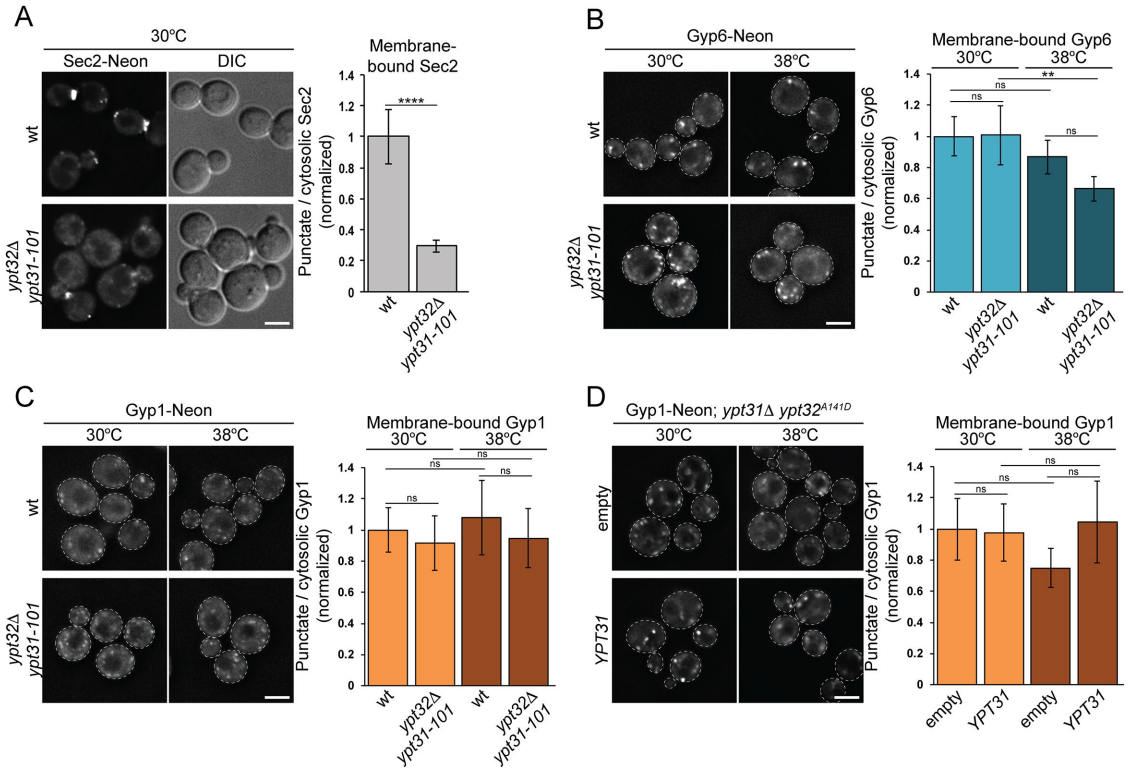

FIGURE 4: Ypt31/32 does not appear to be critical for Gyp1 or Gyp6 recruitment. (A) Left: Representative images of endogenous Sec2-mNeonGreen in wild-type cells versus a *ypt32*Δ *ypt31-101* mutant grown at 30°C. Right: Quantification of punctate (membrane-associated) versus cytosolic Sec2 derived from the images at left. Error bars represent 95% CI for $n \geq 16$ puncta. (B) Left: Representative images of endogenous Gyp6-mNeonGreen in wild-type cells versus a *ypt32*Δ *ypt31-101* mutant grown at 30°C or after shifting to 38°C for 20 min. Right: Quantification of membrane-associated versus cytosolic Gyp6 derived from the images at left. Error bars represent 95% CI for $n \geq 16$ puncta. (C) Left: Representative images of endogenous Gyp1-mNeonGreen in wild-type cells versus a *ypt32*Δ *ypt31-101* mutant grown at 30°C or after shifting to 38°C for 20 min. Right: Quantification of membrane-associated versus cytosolic Gyp1 derived from the images at left. Error bars represent 95% CI for $n \geq 16$ puncta. (D) Left: Representative images of plasmid-borne Gyp1-mNeonGreen in a *ypt31*Δ *ypt32*A141D mutant grown at 30°C or after shifting to 38°C for 20 min. Cells were transformed with empty vector or rescued with wild-type *YPT31* as indicated. Right: Quantification of membrane-associated versus cytosolic Gyp1 derived from the images at left. Error bars represent 95% CI for $n \geq 21$ puncta. Scale bars, 2 μm. n.s., not significant; **, $P < 0.01$; ****, $P < 0.0001$.

confirms that Ypt31/32 is an important Sec2 recruiter and that overexpression of GTP-locked Ypt31(Q72L) can be used to identify major Ypt31/32 effectors.

We found that overexpression of either wild-type Ypt31 or Ypt31(Q72L) did not restore Gyp1 or Gyp6 localization following MNTC treatment (Figure 5, B and C, and Supplemental Figure S5, C and D). We also tested whether wild-type or GTP-locked Ypt31 might rescue Gyp6 localization in a *trs130Δ33* mutant or Gyp1 localization in an *arf1*Δ mutant, but no rescue was observed in either case (Supplemental Figure S6, A and B). Overall, these results suggest that Ypt31/32 is comparatively less important than Arf1 or TRAPPII in localizing Gyp1 and Gyp6 to the Golgi in vivo.

Arf1 and Ypt31/32 bind distinct Gyp1 domains

A previous study mapped the Ypt31/32 binding domain to the N-terminal 210 residues of Gyp1 (Figure 5D) (Rivera-Molina and Novick, 2009). Conservation analysis reveals that this domain represents the least-conserved region among Gyp1 homologues (Lafourcade *et al.*, 2004). This lack of conservation provides support for the idea that interaction with Ypt31/32 might not be essential for Gyp1 function. To explore this hypothesis, we tested whether truncated $Gyp1_{239\text{-}637}$ could complement a *gyp1*Δ mutation, which causes reduced cell growth at elevated temperatures (Du and Novick, 2001). $Gyp1_{239\text{-}637}$, which lacks the Ypt31/32 binding domain but retains the catalytic Rab-GAP domain (Albert *et al.*, 1999; Rak *et al.*, 2000), fully rescued cell growth in the *gyp1*Δ mutant (Figure 5E). This is consistent with previous studies reporting that the Gyp1 N-terminus is dispensable for activity (Du and Novick, 2001; Lafourcade *et al.*, 2004) and indicates that association with Ypt31/32 is not required for Gyp1 function in maintaining cell viability at elevated temperatures.

We next examined the localization of mNeonGreen-tagged $Gyp1_{239\text{-}637}$ relative to TRAPPII-labeled late Golgi/TGN compartments. In agreement with previous findings (Rivera-Molina and Novick, 2009), we found that the N-terminal truncation partially mislocalizes Gyp1 to the cytosol (Supplemental Figure S6, C and D). As described above (see Figure 2, D and E), we found that an extra copy of *ARF1* enhances membrane association of full-length Gyp1. Arf1 overexpression similarly rescued $Gyp1_{239\text{-}637}$ membrane binding (Supplemental Figure S6, C and D), suggesting that the Arf1 binding site resides in the Gyp1 C-terminus. Additionally, we noticed that, although $Gyp1_{239\text{-}637}$ was able to partially associate with membranes, it overlapped poorly with TRAPPII-labeled late Golgi/TGN compartments (Supplemental Figure S6, C and D). This raises

the possibility that Arf1 mediates the initial association of Gyp1 with early/medial Golgi compartments and that Ypt31/32 is required to stabilize Gyp1 at the TGN through interaction with the Gyp1 N-terminal domain. Therefore $Gyp1_{239\text{-}637}$, which lacks the Ypt31/32 binding domain, is poorly retained at Golgi compartments and does not overlap extensively with TRAPPII.

Finally, we used in vitro membrane-binding assays to test whether Arf1 directly recruits $Gyp1_{239\text{-}637}$ to TGN-like liposomes. In agreement with our in vivo findings, activated Arf1 enhanced membrane association of $Gyp1_{239\text{-}637}$ (Supplemental Figure S6E), indicating that the Arf1 binding site resides in the Gyp1 C-terminus. However, $Gyp1_{239\text{-}637}$ bound membranes relatively weakly as compared with full-length $Gyp1_{1\text{-}637}$, suggesting that the Gyp1 N-terminus also contributes to robust membrane association by enhancing the interaction with either lipids or Arf1.

Arf1 and TRAPPII regulate Ypt1 and Ypt6 inactivation by Gyp1 and Gyp6

We next asked whether TRAPPII and Arf1 recruitment of Gyp6 and Gyp1 serves to regulate inactivation of their substrate Rab GTPases Ypt6 and Ypt1. To measure Rab inactivation in cells, we used localization as a proxy for Rab activity: activated Ypt6 and Ypt1 are targeted to the Golgi, whereas inactive Rabs are cytosolic/ER localized (Cabrera and Ungermann, 2013). We first examined whether TRAPPII is required for efficient Ypt6 inactivation. We used anchor away to conditionally recruit TRAPP complexes to the PM, thus depleting TRAPPII from the Golgi. In control experiments, TRAPP anchor away impaired activation of its substrate Ypt32 (Supplemental Figure S7B), indicating that this method effectively depletes TRAPPII from the Golgi. In contrast, we found that TRAPPII anchor away significantly enhanced Ypt6 accumulation at Golgi compartments (Figure 6A), consistent with TRAPPII functioning in Ypt6 inactivation by positively regulating Gyp6. Given that TRAPP anchor away also impairs Ypt31/32 activation, we note that this experiment does not distinguish between the roles of TRAPPII versus Ypt31/32 in directly regulating Gyp6.

To examine whether Arf1-dependent Rab-GAP recruitment to the Golgi drives Ypt1 and Ypt6 inactivation, we monitored Rab activation in MNTC-treated cells. Consistent with our observation that MNTC induces Gyp6 and Gyp1 mislocalization (see Figure 2), we found that active Ypt6 and Ypt1 accumulated at Golgi compartments in MNTC-treated cells (Figure 6, B and C). Ypt6 and Ypt1 showed increased overlap with the late Golgi/TGN marker Sec7, indicating that both Rabs remain activated at the Golgi longer in MNTC-treated cells. These findings are consistent with previous studies reporting that both Ypt6 and Ypt1 remain at the Golgi later upon loss of Gyp6 or Gyp1 function, respectively (Rivera-Molina and Novick, 2009; Suda *et al.*, 2013; Kawamura *et al.*, 2014).

Finally, we tested whether the recruitment of the Rab-GAPs by TRAPPII and Arf1 results in Rab inactivation on liposomes in vitro. We generated prenylated Rab/GDI substrates (Supplemental Figure S7C) and developed a membrane extraction assay to measure Rab inactivation in vitro. In our membrane extraction assay, prenylated Rab/GDI is activated in the presence of liposomes, causing transfer of the Rab from its GDI chaperone to the membrane (Müller and Goody, 2018). GAP-mediated Rab inactivation results in reextraction by the GDI; therefore the amount of membrane-bound Rab can be used as an inverse measure of GAP activity (Figure 6D). In initial experiments, we found that 10 nM Gyp1 can fully inactivate 1 µg of prenylated Ypt1 on TGN liposomes (Supplemental Figure S7D). However, at lower concentrations Gyp1 required additional membrane recruitment to facilitate robust Ypt1 inactivation: we found that the addition of Arf1 enabled 0.5 nM Gyp1 to efficiently inactivate Ypt1 (Figure 6, E–G). In control experiments, Ypt1 loaded with the nonhydrolyzable GTP analogue GMP-PNP remained largely membrane-bound (Figure 6, F and G), indicating that membrane extraction by GDI required Gyp1-catalyzed GTP hydrolysis. Taken together, our data indicate that Arf1 can drive Ypt1 inactivation in vitro by directly recruiting Gyp1.

Using GAP titration experiments, we found that 0.5 nM Gyp6 was sufficient to inactivate Ypt6 (Supplemental Figure S7E), consistent with our observation that Gyp6 alone displays relatively high affinity for TGN membranes (Supplemental Figure S4D). At concentrations lower than 0.1 nM, Gyp6 required additional factors to facilitate Ypt6 inactivation. The addition of recombinant TRAPPII (rTRAPPII), recruited by Arf1, significantly enhanced Gyp6-mediated Ypt6 inactivation (Figure 6, H and I), supporting a model in which TRAPPII recruits Gyp6 to drive Ypt6 inactivation. While testing the role of TRAPPII in Gyp6-mediated Ypt6 inactivation in vitro, we found that TRAPPII purified from yeast cells caused full membrane extraction of Ypt6 in the absence of purified Gyp6, whereas rTRAPPII did not (Supplemental Figure S7, F and G). We hypothesize that the observed Ypt6 GAP activity of TRAPPII results from a substoichiometric amount of Gyp6 copurifying with endogenous TRAPPII. Indeed, a previous study found that Gyp6 copurified with TRAPPII isolated from yeast (Brunet *et al.*, 2016). Taken together, our results provide strong additional support for a model in which TRAPPII physically interacts with Gyp6 to mediate Ypt6 inactivation at the late Golgi.

Arf1 and TRAPPII remodel the Rab composition of the TGN

Previous studies have found that Ypt6 and Ypt1 remain at the TGN later in *gyp6*Δ and *gyp1*Δ mutants, respectively, indicating that GAP activity controls Rab dynamics on maturing Golgi compartments (Rivera-Molina and Novick, 2009; Suda *et al.*, 2013). Therefore, if TRAPPII and Arf1 coordinate Rab inactivation at the TGN, we expect that Ypt6 and Ypt1 would remain at the Golgi later in TRAPPII and Arf1 mutants. To test this hypothesis, we used time-lapse imaging to observe Rab dynamics in *arf1*Δ and *trs130*Δ*33* mutants. We first confirmed that Ypt6 localization to the late Golgi/TGN was enhanced in both mutants (Figure 7A), consistent with a previous study as well as our observation that Gyp6 is mislocalized in both *arf1*Δ and *trs130*Δ*33* cells (see Figure 2C) (Brunet *et al.*, 2016). Ypt1 accumulation at the TGN was also specifically enhanced in the *arf1*Δ mutant (Figure 7B), again consistent with our observation that Gyp1 is mislocalized in *arf1*Δ cells (see Figure 2D).

In wild-type cells, Ypt6 levels declined at the late Golgi/TGN as Sec7 began to accumulate; therefore there was relatively little overlap between these two proteins (Figure 7C). In the *arf1*Δ and *trs130*Δ*33* mutants, Ypt6 inactivation and extraction was delayed, resulting in increased overlap between Ypt6 and Sec7. Ypt1 remained at the TGN later than Ypt6, yet still began to decline before Sec7 reached peak accumulation in wild-type cells (Figure 7C). The timing of Ypt1 was unaffected in the *trs130*Δ*33* mutant, providing further evidence that TRAPPII does not play a role in regulating Ypt1 dynamics. In the *arf1*Δ mutant, Ypt1 showed very little decline and often remained at the TGN during terminal vesiculation, indicating that Arf1 is critical for Ypt1 inactivation (Figure 7C). Our findings are consistent with prior reports demonstrating that GAP activity drives extraction of Rab substrates (Rivera-Molina and Novick, 2009; Suda *et al.*, 2013) and suggest that Arf1 and TRAPPII regulate Ypt1 and Ypt6 dynamics through recruitment of Gyp1 and Gyp6.

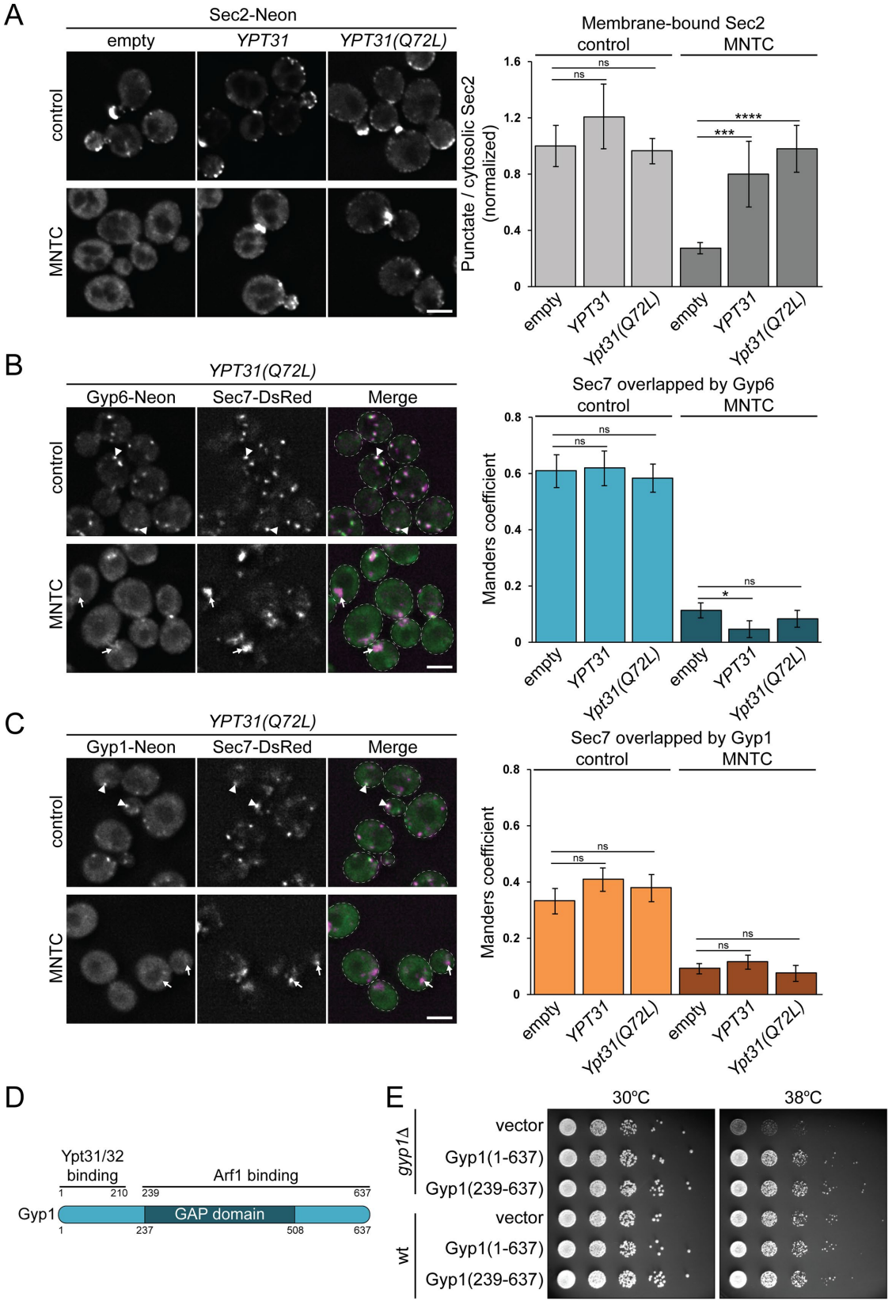

FIGURE 5: Interaction with Ypt31/32 does not appear to be required for Gyp1 function. (A) Left: Representative images of Sec2 in untreated cells versus cells treated with the Sec7 inhibitor MNTC (20 μM, 15 min). Cells are transformed with empty vector or a 2 μm plasmid containing wild-type or GTP-locked *YPT31(Q72L)* as indicated. Right: Quantification of punctate (membrane-associated) versus cytosolic Sec2 derived from the images at left. Error bars represent 95% CI for $n \geq 14$ puncta. (B) Left: Representative images of Gyp6 recruitment to Sec7-labeled late Golgi/TGN compartments in untreated versus MNTC-treated cells (20 μM, 15 min). All cells are expressing plasmid-borne GTP-locked Ypt31(Q72L).

Taken together, our data support a model in which Arf1 and TRAPPII mediate a sharp transition from Ypt1 and Ypt6 to Ypt31/32 at the TGN. Loss of Arf1 or TRAPPII function prolongs Ypt1 and Ypt6 residence at the TGN, thus disrupting Rab conversion and blurring distinct Rab domains.

DISCUSSION

Rab GTPases are essential mediators of membrane transport and organelle identity; therefore it is critical that Rab activity be precisely controlled. While the regulation of Rab-GEF subcellular targeting and activity has been relatively well-studied, comparatively less is known regarding the signals that influence Rab-GAP localization and activity. Prior studies have found that countercurrent GAP cascades play a role in Rab conversion at the late Golgi/TGN and have proposed that TGN-localized Ypt31/32 recruits both Gyp1 and Gyp6 to inactivate the earlier-acting Rabs Ypt1 and Ypt6 (Rivera-Molina and Novick, 2009; Suda *et al.*, 2013). In this present study, we provide evidence that three additional factors contribute to GAP recruitment to drive efficient inactivation of Ypt1 and Ypt6 at the late Golgi: Arf1, the TRAPPII complex, and membrane lipid composition.

We propose an updated model describing the coordination of Rab conversion at the TGN (Figure 7D). At the early/medial Golgi, the GEFs TRAPPIII and Ric1/Rgp1 activate and stabilize Ypt1 and Ypt6, respectively, while Gea1/2 activates Arf1 (Peyroche *et al.*, 1996; Siniossoglou *et al.*, 2000; Spang *et al.*, 2001; Pusapati *et al.*, 2012; Thomas *et al.*, 2018). Arf1 initiates Gyp1 recruitment, yet Ypt1 remains present at Golgi membranes due to continued activation by TRAPPIII. As Golgi compartments mature, the late Golgi Arf-GEF Sec7 continues to activate Arf1, and Golgi membranes become progressively enriched with anionic phospholipids (Bigay and Antonny, 2012; Platre *et al.*, 2018). Arf1 cooperates with these anionic lipids to recruit TRAPPII (Thomas and Fromme, 2016), which initiates Gyp6 recruitment and activates Ypt31/32. Activated Ypt31/32 then cooperates with Arf1 and TRAPPII to stabilize Gyp1 and Gyp6 at the TGN. At this stage, TRAPPIII and Ric1/Rgp1 are no longer present at the TGN, and therefore Gyp1 and Gyp6 efficiently inactivate Ypt1 and Ypt6 to drive a sharp conversion to a Ypt31/32 domain. We also found that both Gyp1 and Gyp6 possess affinity for TGN-like membranes and were not recruited to simple PC liposomes. This indicates that membrane composition is important for recruitment of these two Rab-GAPs and is reminiscent of prior studies showing that both membrane curvature and negative charge mediate recruitment of the Arf-GAP Gcs1 to the TGN (Bigay *et al.*, 2003; Xu *et al.*, 2013).

In support of a role for Arf1 and TRAPPII in coordinating Rab inactivation, we found that Gyp1 and Gyp6 were severely mislocalized in Arf1 and TRAPPII mutants, respectively. Consequently, Ypt1 and Ypt6 remained at Golgi compartments later in these mutants, consistent with prior studies demonstrating prolonged Ypt1 and Ypt6 activity upon loss of GAP function (Rivera-Molina and Novick, 2009; Suda *et al.*, 2013). Owing to extensive cross-talk among membrane transport pathways, we could not discern the precise relative contribution of Arf1 and TRAPPII in Rab-GAP recruitment in vivo. However, our in vitro membrane-binding and Rab extraction assays indicate that Arf1 and TRAPPII can directly recruit Gyp1 and Gyp6 to drive Ypt1 and Ypt6 inactivation, respectively. Interestingly, we also found that Arf1 enhanced Gyp6 membrane association in vitro, which raised the possibility that Arf1 plays an additional role in Ypt6 inactivation. However, Gyp6 was only weakly mislocalized in *arf1*Δ mutant cells, and Arf1 overexpression did not enhance Gyp6 membrane binding in vivo. In comparison, Gyp6 was nearly completely mislocalized in TRAPPII mutants and could not be rescued by an extra copy of *ARF1*. Therefore, while it remains possible that Arf1 contributes to Gyp6 localization, on balance our data support a model in which TRAPPII is the more important Gyp6 recruiter, consistent with a previous report from the Sacher lab (Brunet *et al.*, 2016).

Overall, our results indicate that Ypt31/32 is not required for initial recruitment of Gyp1 or Gyp6 to the Golgi complex. We found that Gyp1 was present at early/medial compartments and that Gyp6 recruitment to the late Golgi peaked before peak Ypt31/32 activation at the TGN. Previous studies report that approximately 40% of Gyp1 and Gyp6 puncta do not contain Ypt31/32 (Rivera-Molina and Novick, 2009; Suda *et al.*, 2013), which may represent earlier compartments that have not yet acquired Ypt31/32. Furthermore, we found that Gyp1 and Gyp6 were more severely mislocalized in Arf1 and TRAPPII mutants, respectively, as compared with Ypt31/32 mutants. This finding is in agreement with the report that Ypt6 inactivation was more impaired in a TRAPPII mutant in comparison to a Ypt31/32 mutant (Brunet *et al.*, 2016) and suggests that TRAPPII is more important for Gyp6 recruitment than is Ypt31/32. Moreover, our in vitro membrane-binding assays indicate that Arf1 and TRAPPII are stronger recruiters of Gyp1 and Gyp6 when directly compared with Ypt31/32.

We propose that Ypt31/32 cooperates with Arf1 and TRAPPII to stabilize GAP localization at the TGN. This is supported by our finding that $Gyp1_{239\text{-}637}$, which lacks the predicted Ypt31/32 binding domain, overlaps less with the TGN as compared with full-length Gyp1. Furthermore, our truncation analyses suggest that Arf1 and Ypt31/32 bind distinct Gyp1 domains, raising the possibility that both GTPases might interact simultaneously to reinforce Gyp1 membrane association. Other effectors have been shown to be

Right: Quantification of Gyp6 recruitment to Sec7-labeled compartments measured using the Manders overlap coefficient. Cells are transformed with empty vector or a 2 μm plasmid containing wild-type or GTP-locked *YPT31(Q72L)* as indicated. See Supplemental Figure S5C for representative images of cells transformed with empty vector or wild-type *YPT31*. Error bars represent 95% CI for $n > 25$ cells. (C) Left: Representative images of Gyp1 recruitment to Sec7-labeled late Golgi/TGN compartments in untreated versus MNTC-treated cells (20 μM, 15 min). All cells are expressing plasmid-borne GTP-locked Ypt31(Q72L). Right: Quantification of Gyp1 recruitment to Sec7-labeled compartments. Cells are transformed with empty vector or a 2 μm plasmid containing wild-type or GTP-locked *YPT31(Q72L)* as indicated. See Supplemental Figure S5D for representative images of cells transformed with empty vector or wild-type *YPT31*. Error bars represent 95% CI for $n > 25$ cells. (D) Schematic depicting domain architecture of Gyp1. Ypt31/32 is reported to bind the N-terminal 210 residues of Gyp1 (Rivera-Molina and Novick, 2009). (E) Plasmid-borne full-length Gyp1(1-637) and Gyp1(239-637) were tested for their ability to rescue temperature sensitivity in a *gyp1*Δ mutant. Note that Gyp1(239-637) lacks the predicted N-terminal Ypt31/32 binding domain. Scale bars, 2 μm. White arrowheads and arrows denote colocalization or a lack of colocalization of tagged proteins at Golgi compartments, respectively. n.s., not significant; *, $P < 0.05$; ***. $P < 0.001$; ****, $P < 0.0001$.

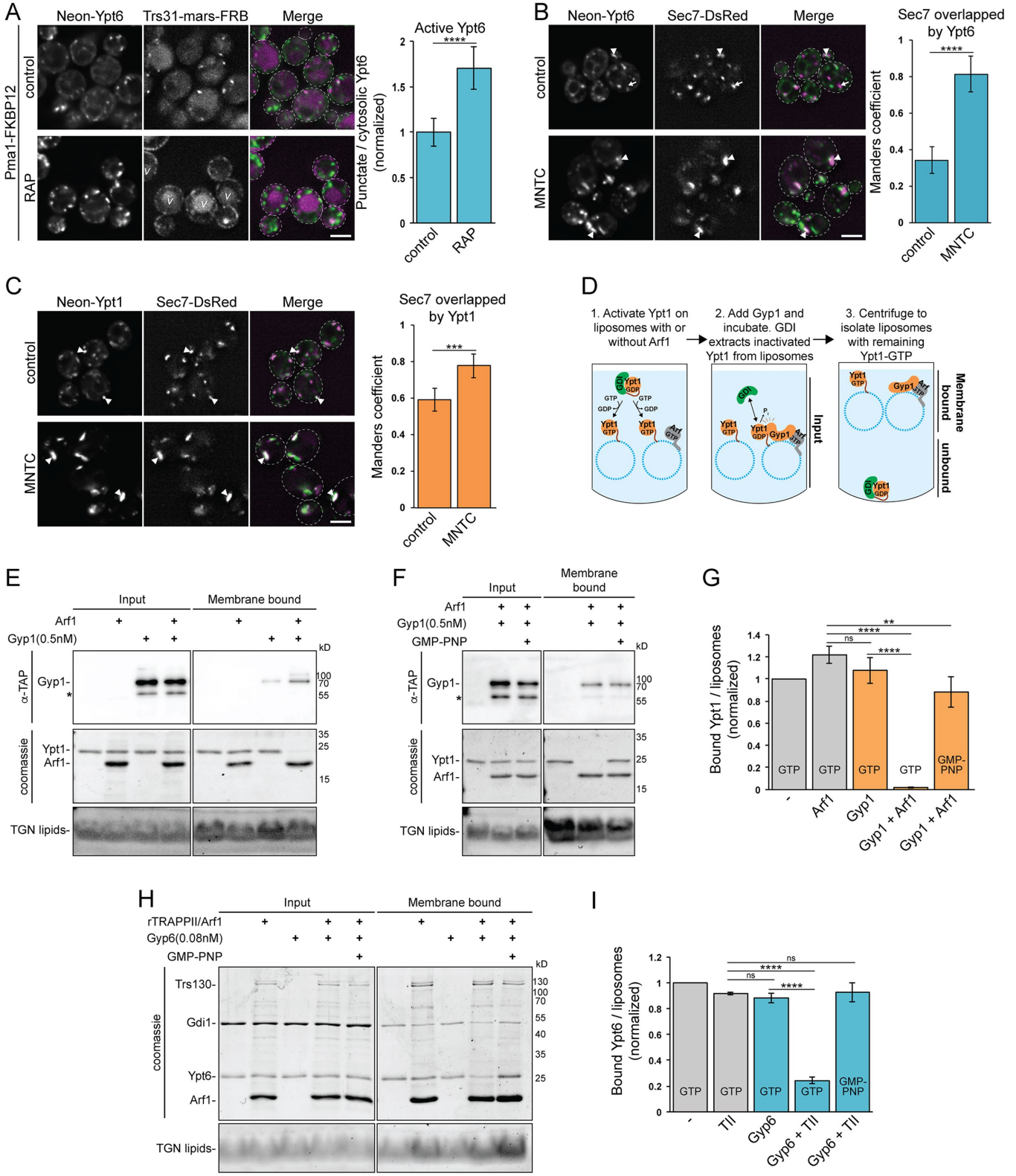

FIGURE 6: TRAPPII and Arf1 recruit Gyp6 and Gyp1 to inactivate Ypt6 and Ypt1, respectively. (A) Left: Representative images showing localization of plasmid-borne mNeonGreen-Ypt6 in untreated cells versus cells with TRAPP complexes relocalized to the PM via rapamycin (RAP)-induced association with Pma1-FKBP12. Right: Quantification of punctate (active) versus cytosolic (inactive) Ypt6 derived from the images at left. Error bars represent 95% CI for $n \geq 18$ puncta. "v" = vacuolar signal; this occurs as an artifact for some RFP-tagged proteins and is not relevant to the study. (B) Left: Representative images of plasmid-borne mNeonGreen-Ypt6 localization/activation at Sec7-labeled late Golgi/TGN compartments in untreated cells versus cells treated with the Sec7 inhibitor MNTC (20 μM, 15 min). Right: Quantification of Ypt6 recruitment/activation at Sec7-labeled compartments measured using the Manders overlap coefficient. Error

recruited by multiple distinct GTPases, which likely promotes robust membrane binding as well as coordination between distinct membrane transport pathways (Rai *et al.*, 2019). Brunet *et al.* (2016) proposed that TRAPPII recruits Gyp6 by cooperating with Ypt31/32 in a positive-feedback loop: TRAPPII recruits Gyp6 and also activates Ypt31/32, which further stabilizes Gyp6 membrane binding. In both cases, GAP binding to Ypt31/32 could function as a fail-safe mechanism to ensure that Ypt1 and Ypt6 are extracted from the Golgi as secretory vesicles form.

Precise termination of Rab activity is critical in maintaining organelle identity and fidelity of transport pathways. GAP mutants cause prolonged Rab activity and residence at target organelles, resulting in ectopic localization of effector proteins (Rivera-Molina and Novick, 2009; Lachmann *et al.*, 2012). For example, *gyp1*Δ mutants display cell growth and trafficking defects that are exacerbated by Ypt1 overexpression (Du and Novick, 2001; Lafourcade *et al.*, 2004), underscoring the importance of regulated Ypt1 inactivation. In a recent study, incorrect targeting of a Ypt1 effector to secretory vesicles prevented vesicle docking to the PM (Yuan *et al.*, 2017), indicating that Rab inactivation must be precisely controlled to prevent deleterious ectopic localization of Rab effectors. Accordingly, we find that Rab inactivation at the TGN is more complex than previously described and involves the coordinated and direct action of at least four factors: Arf1, the TRAPPII complex, Ypt31/32, and the lipid composition of TGN membranes. Arf1 plays a major role in TRAPPII recruitment, and thus Ypt31/32 activation; we therefore propose that Arf1 is a key driver of Rab conversion on maturing Golgi compartments.

MATERIALS AND METHODS

Yeast strains and plasmids

All yeast strains and plasmids used in this study were generated using standard techniques and are listed in Supplemental Tables S1 and S2, respectively. Yeast strains expressing tandem affinity purification (TAP)-tagged Trs130, Sec7, and GAPs were purchased from Dharmacon. *ypt32*Δ *ypt31-101* and *ypt31*Δ *ypt32*A141D mutant strains have been previously described (Jedd *et al.*, 1997; Sciorra *et al.*, 2005). A target of rapamycin (TOR) pathway mutant expressing Pma1-2xFKBP (Auffarth *et al.*, 2014) was used for anchor-away experiments. All other yeast strains were derived from the haploid *Saccharomyces cerevisiae* strains SEY6210 (*MAT*α) and SEY6210.1 (*MAT*a) with genotype *ura3-52 his3-*Δ*200 leu2-3,112 lys2-801 trp1-*Δ*901 suc2-*Δ*9* (Robinson *et al.*, 1988). Yeast were grown in yeast extract, peptone, dextrose (YPD) or synthetic dropout (SD) media at 30°C and analyzed in log phase (OD_{600} of ~0.5).

For most strains, genetic manipulation was carried out using homologous recombination of PCR-amplified cassettes (Longtine *et al.*, 1998). Endogenous *TRS130*, *GYP1*, *GYP6*, *GYP2*, and *SEC2* were tagged at their C-termini with a *mNeonGreen::HIS3* cassette. *TRS130* and *GEA1* were tagged at their C-termini with a *3xmRFPmars::TRP1* cassette. To deplete TRAPP complexes from the Golgi, the TRAPP core subunit *TRS31* was tagged at the C-terminus with a *mRFPmars-FRB::HIS3* cassette. Deletion mutants were generated by replacing gene-coding regions with a *KanMX*, *HIS3*, or *TRP1* cassette. *SEC7* was tagged with *6xDsRed* at the C-terminus using an integration plasmid (Losev *et al.*, 2006), and *ARF1-msGFP* was integrated as an extra copy using an integration plasmid (Day *et al.*, 2018). All tagged strains grew normally, and localization of fluorescent proteins is consistent with previously published studies. The mNeonGreen tag does not interfere with Gyp1 function as Gyp1-mNeonGreen rescues temperature sensitivity in a *gyp1*Δ mutant (Figure 5E). *gyp6*Δ and *gyp2*Δ mutants do not cause growth or temperature sensitivity defects (Sciorra *et al.*, 2005; Kawamura *et al.*, 2014; Supplemental Figure S1C); therefore we were not able to test whether a C-terminal mNeonGreen tag affects Gyp6 or Gyp2 functionality. However, the localization of Gyp6- and Gyp2-mNeonGreen is consistent with that of tagged Gyp6 and Gyp2 used in prior studies (Lafourcade *et al.*, 2003; Suda *et al.*, 2013; Kawamura *et al.*, 2014). Furthermore, Gyp6-TAP is functional in GAP activity assays (Figure 6, H and I, and Supplemental Figure S7E), indicating that a C-terminal tag does not abolish Gyp6 activity.

bars represent 95% CI for $n > 30$ cells. (C) Left: Representative images of plasmid-borne mNeonGreen-Ypt1 localization/activation at Sec7-labeled late Golgi/TGN compartments in untreated cells versus cells treated with the Sec7 inhibitor MNTC (20 μM, 15 min). Right: Quantification of Ypt1 recruitment/activation at Sec7-labeled compartments measured using the Manders overlap coefficient. Error bars represent 95% CI for $n > 27$ cells. (D) Schematic depicting the in vitro GAP activity assay used to test the role of Arf1 in Gyp1-mediated Ypt1 inactivation: 1) Prenylated Ypt1 was activated on TGN-like liposomes with or without myristoylated Arf1 via EDTA-mediated nucleotide exchange with excess GTP (or GMP-PNP in control reactions). Ypt1 activation caused transfer of the Rab from the GDI chaperone to the membrane. 2) Gyp1 was added and reactions incubated to allow for membrane recruitment and resulting Ypt1 inactivation. GDI extracted inactivated Ypt1 from liposomes. 3) Liposomes and bound protein were separated from unbound protein via centrifugation. Membrane-bound Ypt1 represents active Rab, whereas inactivated Ypt1 is extracted by GDI and therefore soluble. A similar assay was also used to test the role of TRAPPII Gyp6-mediated Ypt6 inactivation. (E) GAP activity assay testing the role of Arf1 recruitment in Gyp1-mediated Ypt1 inactivation. TGN liposomes were loaded with activated Ypt1-GTP with or without Arf1. Gyp1 was added at a final concentration of 0.5 nM, and Ypt1 inactivation and membrane extraction was assayed via liposome flotation. Arf1 enhances Gyp1 membrane recruitment, thereby mediating Ypt1 inactivation and membrane extraction. Gyp1 was visualized by Western blot; * = Gyp1 degradation product. (F) GAP activity assay testing whether GTP hydrolysis is required for Ypt1 membrane extraction. Ypt1 and Arf1 were activated with GTP or GMP-PNP, a nonhydrolyzable GTP analogue. Gyp1 was added at a final concentration of 0.5 nM, and Ypt1 inactivation and membrane extraction was assayed via liposome flotation. Gyp1 was visualized by Western blot; * = Gyp1 degradation product. (G) Quantification of membrane-associated (active) Ypt1 from reactions in panels E and F. Error bars represent 95% CI for $n \geq 3$ replicate reactions. (H) Representative GAP activity assay testing the role of TRAPPII in Gyp6-mediated Ypt6 inactivation. TGN liposomes were loaded with activated Ypt6-GTP or -GMP-PNP with or without rTRAPPII/Arf1. Gyp6 was added at a final concentration of 0.08 nM, and Ypt6 inactivation and membrane extraction was assayed via liposome flotation. (I) Quantification of membrane-associated (active) Ypt6 from reactions in panel H. TII = rTRAPPII. Error bars represent 95% CI for $n = 3$ replicate reactions. Scale bars, 2 μm. White arrowheads and arrows denote colocalization or a lack of colocalization of tagged proteins at Golgi compartments, respectively. **, $P < 0.01$; ***, $P < 0.001$; ****, $P < 0.0001$.

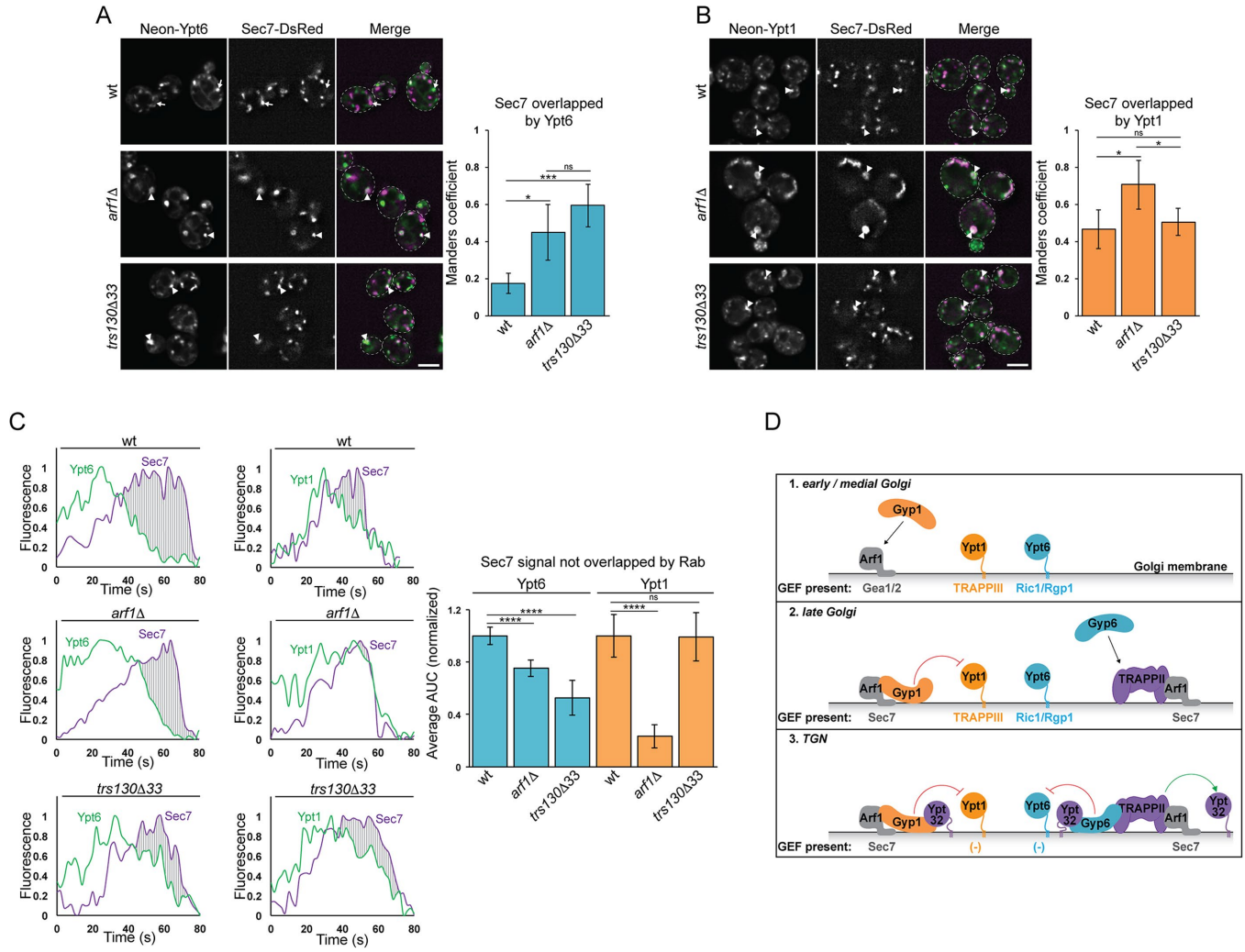

FIGURE 7: Arf1 is a master regulator of Rab conversion during Golgi maturation. (A) Left: Representative images of plasmid-borne mNeonGreen-Ypt6 localization relative to Sec7-labeled late Golgi/TGN compartments in wild-type versus *arf1*Δ and *trs130*Δ*33* (TRAPPII) mutants. Right: Quantification of Ypt6 recruitment/activation at Sec7-labeled compartments measured using the Manders overlap coefficient. Error bars represent 95% CI for $n > 28$ cells. (B) Left: Representative images of plasmid-borne mNeonGreen-Ypt1 localization relative to Sec7-labeled late Golgi/TGN compartments in wild-type versus *arf1*Δ and *trs130*Δ*33* mutants. Right: Quantification of Ypt1 recruitment/activation at Sec7-labeled compartments. Error bars represent 95% CI for $n > 28$ cells. (C) Left: Representative traces from time-lapse imaging series of Ypt6 and Ypt1 versus Sec7 at maturing Golgi compartments. Traces represent normalized quantification of mNeonGreen-Rab and Sec7-6xDsRed signal from single Golgi compartments. Shaded regions highlight time points where the Sec7 signal is greater than that of the Rab. Right: The extent of overlap between Sec7 and each indicated Rab was measured from the traces at left. Error bars represent 95% CI for $n \geq 9$ time-lapse series. (D) Model depicting the role of Arf1, TRAPPII, and Ypt31/32 in Rab conversion at the late Golgi/TGN): 1) At the early/medial Golgi the ArfGEFs Gea1/2 activate Arf1, initiating Gyp1 recruitment. Ypt1 and Ypt6 are activated by TRAPPIII and Ric1/Rgp1, respectively. 2) At the late Golgi, Sec7-activated Arf1 continues to recruit Gyp1 and additionally recruits TRAPPII. TRAPPII in turn initiates Gyp6 recruitment. Ypt1 and Ypt6 activation remains relatively high as their GEFs, TRAPPIII and Ric1/Rgp1, counteract GAP-mediated inactivation. 3) At the TGN TRAPPII activates Ypt31/32, which further stabilizes Gyp1 and Gyp6 membrane binding. The Ypt1 and Ypt6 GEFs are no longer present; therefore both Rabs are efficiently inactivated and removed from the TGN. Ypt1 and Ypt6 inactivation coincident with Ypt31/32 activation drives Rab conversion at the late Golgi/TGN. Scale bars, 2 μm. White arrowheads and arrows denote colocalization or a lack of colocalization of tagged proteins at Golgi compartments, respectively. n.s., not significant; *, $P < 0.05$; ***, $P < 0.001$; ****, $P < 0.0001$.

To visualize Rab localization, cells were transformed with pRS415 containing mNeonGreen-tagged Rabs with the *YPT1* promoter and terminator. Though tagged Rabs were introduced as an extra copy, all mNeonGreen fusions were confirmed using complementation assays to be functional (Thomas *et al.*, 2019; Supplemental Figure S7A). To test whether ectopically localized Arf1 corecruits Gyp1 to the PM, yeast were transformed with pRS423 containing FRB-mRFPmars-ARF1(Q71L)ΔN13 with the high-copy *TDH3* promoter as well as the *CYC1* terminator (pLT1). To explore the role of the Gyp1 N-terminus in localization and function, cells were transformed with pRS415 containing mNeonGreen-tagged Gyp1$_{1\text{-}637}$ or Gyp1$_{239\text{-}637}$ with the *GYP1* promoter and terminator (pLT228 and pLT231).

To test whether an extra copy of *ARF1* rescues GAP localization in various mutants, cells were transformed with pRS415 containing wild-type *ARF1* under the control of its endogenous promoter and terminator (pCF1023). To determine whether increased Ypt31/32 expression rescues Sec2, Gyp6, and Gyp1 mislocalization, cells were transformed with pRS425 containing wild-type *YPT31* or GTP-locked *YPT31(Q72L)* with the *YPT31* promoter and terminator (VSB327 and VSB333; Sciorra *et al.*, 2005). To restore Ypt31/32 function in the *ypt31*Δ *ypt32*A141D mutant, cells were transformed with pRS416 containing wild-type *YPT31* under the control of its endogenous promoter and terminator (VSB283; Sciorra *et al.*, 2005).

Microscopy

Yeast cells were grown overnight (~16 h) in SD media at 30°C and imaged in log phase. Temperature shifts were performed by transferring log-phase yeast cultures to a water bath of the indicated temperature for the indicated time before imaging. Each image shown is a single focal plane. Time-lapse series were generated by imaging a single focal plane every 2 s for 2–4 min. Images were processed using ImageJ, adjusting only the minimum/maximum brightness levels for clarity with identical leveling between all images within a figure panel.

Time-lapse series in Figures 1 and 7 were acquired using a CSU-X spinning-disk confocal system (Intelligent Imaging Innovations) with a DMI6000 B microscope (Leica Microsystems), 100× 1.46 NA oil immersion objective, and a QuantEM electron-multiplying charge-coupled device camera (Photometrics). Series were captured and analyzed using Slidebook 6 software (Intelligent Imaging Innovations). All other images were captured using a DeltaVision Elite system (GE Healthcare) with a 100× 1.35 oil immersion objective and a CoolSNAP HQ2 camera (Photometrics). Images were acquired using softWoRx software (GE Healthcare) and deconvolved (conservative setting; six cycles) to remove out-of-focus light.

MNTC and rapamycin treatment

To test the role of Sec7-activated Arf1 in GAP recruitment to the Golgi, 20 µM of the Sec7 inhibitor 6-methyl-5-nitro-2-(trifluoromethyl)-4*H*-chromen-4-one (MNTC; MolPort compound #MolPort-000-729-160) was added to growth media 15 min before imaging. TRAPP complexes were conditionally depleted from the Golgi by treating cells expressing Trs31-mRFPmars-FRB and Pma1-2xFKBP12 with 1 µg/ml rapamycin (LC Laboratories) 15 min before imaging. To relocalize Arf1-GTP to the PM, cells expressing FRB-mRFPmars-Arf1(Q71L)ΔN13 and Pma1-2xFKBP12 were treated with rapamycin 15 min before imaging.

Image analysis

Manders analysis was used to quantify overlap between GAPs and markers for early and late Golgi compartments. Manders analysis was also used to compare GAP, Rab, and TRAPPII recruitment to the Golgi in different mutants as well as following MNTC treatment. Images were cropped to contain 3–7 cells and analyzed with ImageJ using the JACoP plug-in. Images were thresholded to only quantify signal at Golgi compartments to avoid cytoplasmic background.

Line-scan analysis was used to quantify localization of GAPs, TRAPPII, and Sec7 to endomembrane compartments as well as GTPase activation (membrane binding was used as a proxy for GTPase activity). Using ImageJ, lines traces were chosen to pass through the cytosol and image background as well as the brightest puncta in each cell. For each line trace, the average image background value was subtracted from values obtained for puncta as well as the cytosol. Membrane recruitment and GTPase activation was calculated by dividing the background-subtracted puncta fluorescence by that of the cytosol.

To measure Gyp6 versus Sec7 peak-to-peak recruitment (Figure 1C) as well as the timing of Rab activation in *arf1*Δ and *trs130*Δ*33* mutants (Figure 7C), time-lapse imaging series were analyzed using Slidebook 6 software. For each imaging series, Golgi compartments were chosen that remained distinct from other puncta as well as in the focal plane throughout the entire lifetime of the compartment. The fluorescence intensity of each protein over time was tracked for isolated Golgi compartments and normalized to a value between 0.0 and 1.0. For peak-to-peak measurement, peak recruitment was defined as the time point when the normalized fluorescence = 1.0. To quantify overlap between Rabs and the late Golgi/TGN marker Sec7, normalized Rab fluorescence was subtracted from normalized Sec7 fluorescence, and the area under the curve (AUC) was calculated from the resulting trace.

Cell growth assays

Cell growth assays were conducted to test the temperature sensitivity of the previously characterized *ypt32*Δ *ypt31-101* mutant (Sciorra *et al.*, 2005). Mutant and wild-type yeast were grown on YPD plates at 30°C, and 10–15 freshly grown colonies were resuspended in yeast nitrogen base, diluted to an OD_{600} of 0.6, and then serially diluted onto SD plates. Cells were grown at temperatures ranging from 26°C to 38°C and imaged after 2–3 d. When grown on synthetic media, this mutant was inviable at temperatures greater than 35°C.

To test whether wild-type *YPT31* restores function in the previously described *ypt31*Δ *ypt32*A141D mutant (Jedd *et al.*, 1997), yeast were transformed with empty vector or VSB283 and plated on SD -Ura media. Transformed yeast were assayed for growth on SD -Ura at temperatures ranging from 26°C to 38°C. When grown on synthetic media, this mutant was inviable at temperatures greater than 35°C, and expression of wild-type Ypt31 partially restores growth at temperatures up to 37°C.

To determine whether the Gyp1 N-terminus is required for function, *gyp1*Δ mutants and wild-type cells were transformed with empty vector, pLT228, or pLT231 and plated on SD -Leu media. When grown on synthetic media, the *gyp1*Δ mutant is viable at 30°C but displays reduced growth at temperatures higher than 37°C (Du and Novick, 2001). Restoration of Gyp1 function was therefore assayed by cell growth on SD -Leu at the restrictive temperature of 38°C.

To test the functionality of mNeonGreen-Ypt6, *ypt6*Δ mutant yeast were transformed with empty vector or pLT218 and plated on SD -Leu media. Transformed yeast were assayed for growth on SD -Leu at temperatures ranging from 26°C to 38°C. The *ypt6*Δ mutant is inviable at 38°C, and expression of mNeonGreen-Ypt6 restores growth.

Protein purification

Endogenous GAPs, TRAPPII, and Sec7 were purified from 12–24 l of yeast expressing C-terminal TAP tag fusions. The TAP tag used in this study consists of a calmodulin-binding peptide separated from a protein A tag by a tobacco etch virus (TEV) protease site. Yeast were grown in YPD at 30°C to log phase and then harvested by centrifugation, washed, and resuspended in CHAPS lysis buffer (20 mM HEPES, pH 7.4, 300 mM NaCl, 5% glycerol, 1% CHAPS, 2 mM $MgCl_2$, 1 mM dithiothreitol [DTT]) containing 50 mM NaF, 0.1 mM Na_3VO_4, 1 mM phenylmethylsulfonyl fluoride (PMSF), and 1× protease inhibitor cocktail (Roche). Resuspended cells were flash frozen dropwise in N_2(l) and then lysed while frozen (15 × 2 min cycles) using a freezer mill (SPEX SamplePrep).

The lysate was cleared by centrifugation and incubated with Sepharose 6B (Sigma-Aldrich cat #6B100) for 30 min at 4°C to remove proteins that bind nonspecifically to Sepharose. The cleared lysate was then incubated with immunoglobulin G (IgG) Sepharose (GE Healthcare cat #17096901) for 2–3 h at 4°C to isolate protein A–tagged GAPs or GEFs. The resin was then washed with IPP300 buffer (25 mM Tris-HCl, pH 8.0, 300 mM NaCl, 5% glycerol, 0.1% CHAPS, and 1 mM DTT) followed by TEV cleavage buffer (IPP300 buffer with 0.5 mM EDTA). The washed resin was resuspended in TEV cleavage buffer and nutated overnight at 4°C with TEV protease. Eluted protein was diluted in calmodulin-binding buffer (25 mM Tris-HCl, pH 8.0, 300 mM NaCl, 5% glycerol, 0.1% CHAPS, 1 mM magnesium acetate, 1 mM imidazole, 2 mM $CaCl_2$, and 1 mM DTT) and incubated with Calmodulin Sepharose (GE Healthcare cat #17052901) for 2 h at 4°C. The resin was washed with calmodulin-binding buffer, and purified GAPs, TRAPPII, and Sec7 were eluted using calmodulin elution buffer (25 mM Tris-HCl, pH 8.0, 300 mM NaCl, 5% glycerol, 0.1% CHAPS, 1 mM magnesium acetate, 1 mM imidazole, 20 mM ethylene glycol tetraacetic acid (EGTA), and 1 mM DTT). Eluted fractions were analyzed by SDS–PAGE with Bio-Safe Coomassie (Bio-Rad Laboratories cat #1610786), and fractions containing protein were pooled, flash frozen in N_2(l), and then used in liposome flotation and GAP activity assays.

Recombinant TRAPPII (rTRAPPII) was purified by coexpressing the following three plasmids in Rosetta2 (Novagen cat #71400) cells: a pCOLADuet-1 vector containing the six TRAPP core subunits (*TRS33*, *TRS31*, *TRS23*, *TRS20*, *BET3*, and *BET5*; pLT21), a pETDuet-1 vector containing *TRS120* and *TCA17* (pLT16), and a pCDFDuet-1 vector containing *TRS65* and *TRS130* with a C-terminal TAP tag (pLT36). Gyp1(239-637) was purified from Rosetta2 cells using a pETDuet-1 vector containing *GYP1(239-637)* with a C-terminal TAP tag (pLT232). Cells were grown in 4–8 l terrific broth (TB) at 37°C to an OD_{600} of ~3.0, and then protein expression was induced overnight at 18°C with 300 µM isopropyl thiogalactopyranoside (IPTG). Cells were harvested by centrifugation and lysed by sonication in CHAPS lysis buffer. rTRAPPII and Gyp1(239-637) were purified using an identical protocol as for endogenous TRAPPII. For rTRAPPII, eluted protein was further purified via anion-exchange chromatography using a MonoQ 5/50 GL column equilibrated in calmodulin elution buffer. For Gyp1(239-637), eluted protein was further purified by gel filtration chromatography using a Superdex 200 Increase 10/300 GL column (GE Healthcare) equilibrated with calmodulin elution buffer.

Myristoylated Arf1 and Arl1 were purified by coexpressing Arf1 or Arl1 with the *N*-myristoyl transferase Nmt1 in BL21 (DE3; Novagen cat #69450) cells in the presence of myristate (Sigma-Aldrich cat #M3128). Cells (1–2 l) were grown in Luria–Bertani (LB) broth to an OD_{600} of ~0.6, and then protein expression was induced overnight at 18°C with 1 mM IPTG. Cells were lysed in lysis buffer (20 mM Tris-HCl, pH 8.0, 100 mM NaCl, 1 mM $MgCl_2$, 10 mM β-mercaptoethanol (βME), and 1 mM PMSF), and the lysate was cleared by centrifugation before incubation with DEAE Sephacel (GE Healthcare cat #17050001) to remove major contaminating proteins. The cleared lysate was incubated with phenyl resin (Tosoh Bioscience cat #19818) in high-salt buffer (20 mM Tris-HCl, pH 8.0, 3 M NaCl, 1 mM $MgCl_2$, 1 mM DTT) to isolate hydrophobic myristoylated Arf1. Proteins were eluted with low-salt buffer (20 mM Tris-HCl, pH 8.0, 100 mM NaCl, 1 mM $MgCl_2$, 1 mM DTT) and further purified by gel filtration using a Superdex 200 Increase 10/300 GL column equilibrated with prenylation buffer (20 mM HEPES, pH 7.4, 150 mM NaCl, 2 mM $MgCl_2$, and 1 mM DTT).

Ypt32, Ypt1, Ypt6, and Gdi1 were expressed as N-terminal GST-fusions in Rosetta2 cells. Cells from 1–8 l of TB were lysed in lysis buffer (1× phosphate-buffered saline, 2 mM $MgCl_2$, 5 mM BME, and 1 mM PMSF), and GST-tagged proteins were affinity purified using glutathione resin (G-Biosciences cat #786-310). The resin was washed in lysis buffer followed by PreScission cleavage buffer (50 mM Tris-HCl, pH 7.5, 150 mM NaCl, 1 mM EDTA, 2 mM $MgCl_2$, and 1 mM DTT), and the GST tag was cleaved by nutating overnight at 4°C with PreScission (3C) protease.

Purified Rabs were prenylated in vitro using an enzymatic synthesis procedure as previously described (Thomas and Fromme, 2016). Purified Rabs were loaded with GDP (Sigma-Aldrich cat #G7127) using EDTA-based exchange and then combined with Gdi1, Rab escort protein (His_6-REP), and geranylgeranyl transferase (His_6-GGTase) in a 10:10:1:1 M ratio in prenylation buffer. A sixfold molar excess of geranylgeranyl pyrophosphate (Cayman Chemical cat #63330) was added, and the prenylation reaction was incubated at 37°C for 1 h. His_6-tagged REP and GGTase were removed by incubation with Ni-NTA resin (QIAGEN cat #30210), and prenylated Rab/GDI complexes were further purified by gel filtration with prenylation buffer. Fractions containing stoichiometric complexes were pooled and used as recruiters in liposome flotation assays or substrates in GAP activity assays.

Liposome preparation

With the exception of Supplemental Figure S4E, all experiments were performed with liposome membranes with a lipid composition approximating that of the TGN (Klemm *et al.*, 2009). All liposomes contain 1% DiR near-infrared dye in order to quantify lipid recovery in membrane-binding assays. Individual lipids were combined in the molar ratios described in Supplemental Table S3, vacuum dried, and rehydrated overnight at 37°C in HK buffer (20 mM HEPES, pH 7.4, and 150 mM KOAc). Lipids were extruded using a miniextruder (Avanti Polar Lipids) and filters with a pore size of 100 nm.

Liposome flotation assays

Liposome flotation was used to measure membrane recruitment of GAPs and Sec7. With the exception of Supplemental Figure S4E, all reactions were carried out using TGN-like liposomes. For reactions testing recruitment by GTPases, 5 µg of Arf1, Arl1, or Ypt32 was preactivated on liposome membranes using EDTA-based exchange with the nonhydrolyzable GTP analogue GMP-PNP. For reactions containing TRAPPII, 5 µg of purified TRAPPII was added to liposomes containing Arf1 and incubated at room temperature (RT) for 10 min to allow for TRAPPII membrane binding. Note that TRAPPII requires activated Arf1 to be efficiently recruited to membranes (Thomas and Fromme, 2016). Finally, purified GAP or Sec7 was added to a final concentration of 12 nM and incubated at RT for 15 min to allow for any membrane recruitment.

Liposomes with bound protein were separated from unbound protein using discontinuous sucrose gradient flotation. Each reaction was diluted with HKM buffer (20 mM HEPES, pH 7.4, 150 mM KOAc, 2 mM $MgCl_2$) containing 2.5 M sucrose to a final concentration of 1 M sucrose ("Input" sample). The mixture was transferred to 7 × 20 mm polycarbonate centrifuge tubes (Beckman Coulter cat #343775), overlaid with HKM containing 0.75 M sucrose followed by HKM without sucrose, and centrifuged (390,000 × *g*, 20 min, 20°C). Following centrifugation, liposomes with bound protein were collected from the top layer of the sucrose gradient ("Membrane bound" sample). See Figure 3B for a schematic depicting the liposome flotation procedure.

GAPs and TRAPPII were detected by immunoblotting using an anti-TAP tag antibody; Sec7 was detected using an anti-Sec7 antibody. All GTPases were visualized using Bio-Safe Coomassie;

liposomes were detected using incorporated DiR near-infrared dye. We determined that both Gyp6 and Gyp1 possess intrinsic affinity for TGN membranes and that background binding is reduced by the presence of 0.04% CHAPS detergent (Supplemental Figure S4A). Therefore CHAPS detergent was included to increase stringency in all experiments unless otherwise noted.

ImageJ was used to measure band intensities for GAPs, Arf1, and recovered liposomes in the "Membrane bound" fraction. To quantify GAP recruitment in Figure 3, the amount of bound GAP was normalized to the amount of lipids to control for liposome recovery. In Supplemental Figure S4E, bound GAP was normalized to bound Arf1 to control for liposome recovery and GTPase activation.

GAP activity assays

A modified liposome flotation assay was used to measure Rab membrane extraction as a proxy for GAP activity. To assay Gyp1 activity, 1 µg of prenylated-Ypt1/GDI was preactivated on TGN-like liposomes with or without 5 µg Arf1 using EDTA-based exchange with GTP. Note that Ypt1 activation causes transfer of the Rab from the GDI to the membrane. Gyp1 was then added to a final concentration of 0.5 nM and the reactions incubated at RT for 5 min to allow for Gyp1 membrane recruitment and subsequent Ypt1 inactivation and membrane extraction. Membrane-bound (active) Ypt1 was separated from soluble GDI-bound (inactive) Ypt1 by sucrose gradient flotation as described above. Initial experiments were used to determine that 10 nM Gyp1 is sufficiently recruited to membranes and fully inactivates 1 µg Ypt1 within 5 min (Supplemental Figure S7D). In contrast, 0.5 nM Gyp1 did not bind membranes at sufficient levels and thus required recruitment by Arf1 to mediate Ypt1 inactivation (Figure 6, E–G, and Supplemental Figure S7D). In control experiments, Ypt1 was preactivated with the nonhydrolyzable GTP analogue GMP-PNP. Ypt1-GMP-PNP was not extracted from membranes by the addition of Arf1/Gyp1 (Figure 6, F and G), indicating that membrane extraction can be used as a readout of GTP hydrolysis. See Figure 6D for a schematic depicting the GAP activity assay procedure.

To assay Gyp6 activity, 1 µg of prenylated-Ypt6/GDI was preactivated on TGN-like liposomes with or without 5 µg Arf1 using EDTA-based exchange with GTP or GMP-PNP. Recombinant TRAPPII (rTRAPPII) (5 µg) was added to liposomes containing Arf1 and incubated at RT for 10 min to allow for rTRAPPII membrane binding. Gyp6 was then added to a final concentration of 0.08 nM and the reactions incubated at RT for 5 min to allow for Gyp6 membrane recruitment and subsequent Ypt6 inactivation and membrane extraction. Initial experiments were used to determine that 0.5 nM Gyp6 is sufficiently recruited to membranes and inactivates 1 µg Ypt6 within 5 min (Supplemental Figure S7E). In contrast, <0.1 nM Gyp6 did not bind membranes at sufficient levels and thus required recruitment by rTRAPPII to mediate Ypt6 inactivation (Figure 6, H and I. and Supplemental Figure S7E). ImageJ was used to measure band intensities for Rab GTPases and recovered liposomes in the "Membrane bound" fraction. To quantify Rab membrane extraction in Figure 6, the amount of bound Rab was normalized to the amount of lipids to control for liposome recovery.

While using this assay to test whether TRAPPII recruits Gyp6 to mediate Ypt6 inactivation, we found that the addition of 3 µg TRAPPII purified from yeast efficiently extracted Ypt6 from membranes in the absence of Gyp6 (Supplemental Figure S7G). We suspect that the GAP activity of yeast-purified TRAPPII results from copurifying Gyp6, as rTRAPPII purified from *E. coli* did not inactivate Ypt6.

Antibodies

The anti-TAP tag rabbit polyclonal antibody (Thermo Fisher cat #CAB1001) used to detect TRAPPII and GAPs in liposome flotation assays was used at a 1:1000 dilution. The anti-Sec7 GEF domain rabbit polyclonal antibody used to detect Sec7 in flotation assays was produced using purified recombinant GEF domain from Sec7 as the antigen and used at a 1:1000 dilution. A rabbit IgG horseradish peroxidase–linked secondary (Sigma-Aldrich cat #NA934) was used at a 1:4000 dilution.

Statistical analysis

In all figures error bars represent 95% confidence intervals (CIs). All statistical tests were performed using GraphPad Prism 8 software. For Figures 2, A and B, 4A, 6, A–C, and 7C and Supplemental Figures S1B, S2, S3A, S4, S6E, and S7. significance was determined using an unpaired two-tailed *t* test with Welch's correction. For all other figures, significance was determined using a one-way analysis of variance with Tukey's test for multiple comparisons. For all figures, ns indicates not significant; *, $P < 0.05$; **, $P < 0.01$; ***, $P < 0.001$; ****, $P < 0.0001$.

ACKNOWLEDGMENTS

We thank the laboratories of J. Baskin, A. Bretscher, S. Emr, B. Glick, R. Kahn, N. Segev, and C. Ungermann for generously sharing strains, reagents, equipment, and advice. We are grateful to B. Brownfield and B. Richardson of the Fromme Lab for sharing purified Sec7 and Arl1 protein. We acknowledge E. Sanford and M. Smolka for preliminary analyses of TRAPPII interactors that inspired this study. We thank S. Bagde for critical reading of the manuscript. This work was supported by National Institutes of Health grants R01GM116942 and R35GM136258 to J.C.F.

REFERENCES

Albert Š, Gallwitz D (1999). Two new members of a family of Ypt/Rab GTPase activating proteins: promiscuity of substrate recognition. J Biol Chem 274, 33186–33189.

Albert S, Will E, Gallwitz D (1999). Identification of the catalytic domains and their functionally critical arginine residues of two yeast GTPase-activating proteins specific for Ypt/Rab transport GTPases. EMBO J 18, 5216–5225.

Auffarth K, Arlt H, Lachmann J, Cabrera M, Ungermann C (2014). Tracking of the dynamic localization of the Rab-specific HOPS subunits reveal their distinct interaction with Ypt7 and vacuoles. Cell Logist 4, e29191.

Barr F, Lambright DG (2010). Rab GEFs and GAPs. Curr Opin Cell Biol 22, 461–470.

Bigay J, Antonny B (2012). Curvature, lipid packing, and electrostatics of membrane organelles: defining cellular territories in determining specificity. Dev Cell 23, 886–895.

Bigay J, Gounon P, Robineau S, Antonny B (2003). Lipid packing sensed by ArfGAP1 couples COPI coat disassembly to membrane bilayer curvature. Nature 426, 563–566.

Brunet S, Saint-Dic D, Milev MP, Nilsson T, Sacher M (2016). The TRAPP subunit Trs130p interacts with the GAP Gyp6p to mediate Ypt6p dynamics at the late Golgi. Front Cell Dev Biol 4, 48.

Cabrera M, Ungermann C (2013). Guanine nucleotide exchange factors (GEFs) have a critical but not exclusive role in organelle localization of rab GTPases. J Biol Chem 288, 28704–28712.

Casanova JE (2007). Regulation of Arf activation: the Sec7 family of guanine nucleotide exchange factors. Traffic 8, 1476–1485.

Cherfils J (2014). Arf GTPases and their effectors: assembling multivalent membrane-binding platforms. Curr Opin Struct Biol 29, 67–76.

Day KJ, Casler JC, Glick BS (2018). Budding yeast has a minimal endomembrane system. Dev Cell 44, 56–72.e4.

Donaldson JG, Jackson CL (2011). ARF family G proteins and their regulators: roles in membrane transport, development and disease. Nat Rev Mol Cell Biol 12, 362–375.

Du L-L, Collins RN, Novick PJ (1998). Identification of a Sec4p GTPase-activating protein (GAP) as a novel member of a Rab GAP family. J Biol Chem 273, 3253–3256.

Du L-L, Novick P (2001). Yeast Rab GTPase-activating protein Gyp1p localizes to the Golgi apparatus and is a negative regulator of Ypt1p. Mol Biol Cell 12, 1215–1226.
Halaby SL, Fromme JC (2018). The HUS box is required for allosteric regulation of the Sec7 Arf-GEF. J Biol Chem 293, 6682–6691.
Haruki H, Nishikawa J, Laemmli UK (2008). The anchor-away technique: rapid, conditional establishment of yeast mutant phenotypes. Mol Cell 31, 925–932.
Jedd G, Mulholland J, Segev N (1997). Two New Ypt GTPases are required for exit from the yeast trans-golgi compartment. J Cell Biol 137, 563–580.
Jedd G, Richardson C, Litt R, Segev N (1995). The Ypt1 GTPase is essential for the first two steps of the yeast secretory pathway. J Cell Biol 131, 583–590.
Kawamura S, Nagano M, Toshima JY, Toshima J (2014). Analysis of subcellular localization and function of the yeast Rab6 homologue, Ypt6p, using a novel amino-terminal tagging strategy. Biochem Biophys Res Commun 450, 519–525.
Kim JJ, Lipatova Z, Majumdar U, Segev N (2016). Regulation of golgi cisternal progression by Ypt/Rab GTPases. Dev Cell 36, 440–452.
Klemm RW, Ejsing CS, Surma Ma, Kaiser HJ, Gerl MJ, Sampaio JL, De Robillard Q, Ferguson C, Proszynski TJ, Shevchenko A, *et al*. (2009). Segregation of sphingolipids and sterols during formation of secretory vesicles at the trans-Golgi network. J Cell Biol 185, 601–612.
Knödler A, Feng S, Zhang J, Zhang X, Das A, Peränen J, Guo W (2010). Coordination of Rab8 and Rab11 in primary ciliogenesis. Proc Natl Acad Sci USA 107, 6346–6351.
Lachmann J, Barr FA, Ungermann C (2012). The Msb3/Gyp3 GAP controls the activity of the Rab GTPases Vps21 and Ypt7 at endosomes and vacuoles. Mol Biol Cell 23, 2516–2526.
Lafourcade C, Galan J-M, Gloor Y, Haguenauer-Tsapis R, Peter M (2004). The GTPase-activating enzyme Gyp1p is required for recycling of internalized membrane material by inactivation of the Rab/Ypt GTPase Ypt1p. Mol Cell Biol 24, 3815–3826.
Lafourcade C, Galan J-M, Peter M (2003). Opposite roles of the F-box protein Rcy1p and the GTPase-activating protein Gyp2p during recycling of internalized proteins in yeast. Genetics 164, 469–477.
Liang Y, Morozova N, Tokarev AA, Mulholland JW, Segev N (2007). The role of Trs65 in the Ypt/Rab guanine nucleotide exchange factor function of the TRAPP II complex. Mol Biol Cell 18, 2533–2541.
Longtine MS, McKenzie A, Demarini DJ, Shah NG, Wach A, Brachat A, Philippsen P, Pringle JR (1998). Additional modules for versatile and economical PCR-based gene deletion and modification in Saccharomyces cerevisiae. Yeast 14, 953–961.
Losev E, Reinke CA, Jellen J, Strongin DE, Bevis BJ, Glick BS (2006). Golgi maturation visualized in living yeast. Nature 441, 1002–1006.
McDonold CM, Fromme JC (2014). Four GTPases differentially regulate the Sec7 Arf-GEF to direct traffic at the trans-golgi network. Dev Cell 30, 759–767.
Morozova N, Liang Y, Tokarev AA, Chen SH, Cox R, Andrejic J, Lipatova Z, Sciorra VA, Emr SD, Segev N (2006). TRAPPII subunits are required for the specificity switch of a Ypt–Rab GEF. Nat Cell Biol 8, 1263–1269.
Müller MP, Goody RS (2018). Molecular control of Rab activity by GEFs, GAPs and GDI. Small GTPases 9, 5–21.
Novick P (2016). Regulation of membrane traffic by Rab GEF and GAP cascades. Small GTPases 7, 252–256.
Ortiz D, Medkova M, Walch-Solimena C, Novick P (2002). Ypt32 recruits the Sec4p guanine nucleotide exchange factor, Sec2p, to secretory vesicles; evidence for a Rab cascade in yeast. J Cell Biol 157, 1005–1016.
Peyroche A, Parist S, Jackson CL (1996). Nucleotide exchange on ARF mediated by yeast Gea1 protein. Nature 384, 479–481.
Pfeffer SR (2012). Rab GTPase localization and Rab cascades in Golgi transport. Biochem Soc Trans 40, 1373–1377.
Pfeffer SR (2013). Rab GTPase regulation of membrane identity. Curr Opin Cell Biol 25, 414–419.
Platre MP, Noack LC, Doumane M, Bayle V, Simon MLA, Maneta-Peyret L, Fouillen L, Stanislas T, Armengot L, Pejchar P, *et al*. (2018). A combinatorial lipid code shapes the electrostatic landscape of plant endomembranes. Dev Cell 45, 465–480.e11.
Pusapati GV, Luchetti G, Pfeffer SR (2012). Ric1-Rgp1 complex is a guanine nucleotide exchange factor for the late golgi Rab6A GTPase and an effector of the medial Golgi Rab33B GTPase. J Biol Chem 287, 42129–42137.
Rai A, Goody RS, Müller MP (2019). Multivalency in Rab effector interactions. Small GTPases 10, 40–46.
Rak A, Fedorov R, Alexandrov K, Albert S, Goody RS, Gallwitz D, Scheidig AJ (2000). Crystal structure of the GAP domain of Gyp1p: first insights into interaction with Ypt/Rab proteins. EMBO J 19, 5105–5113.
Richardson BC, McDonold CM, Fromme JC (2012). The Sec7 Arf-GEF is recruited to the trans-golgi network by positive feedback. Dev Cell 22, 799–810.
Rivera-Molina FE, Novick PJ (2009). A Rab GAP cascade defines the boundary between two Rab GTPases on the secretory pathway. Proc Natl Acad Sci USA 106, 14408–14413.
Robinson JS, Klionsky DJ, Banta LM, Emr SD (1988). Protein sorting in Saccharomyces cerevisiae: isolation of mutants defective in the delivery and processing of multiple vacuolar hydrolases. Mol Cell Biol 8, 4936–4948.
Sciorra VA, Audhya A, Parsons AB, Segev N, Boone C, Emr SD (2005). Synthetic genetic array analysis of the PtdIns 4-kinase Pik1p identifies components in a Golgi-specific Ypt31/rab-GTPase signaling pathway. Mol Biol Cell 16, 776–793.
Sclafani A, Chen S, Rivera-Molina F, Reinisch K, Novick P, Ferro-Novick S (2010). Establishing a role for the GTPase Ypt1p at the late Golgi. Traffic 11, 520–532.
Siniossoglou S, Peak-Chew SY, Pelham HRB (2000). Ric1p and Rgp1p form a complex that catalyses nucleotide exchange on Ypt6p. EMBO J 19, 4885–4894.
Spang A, Herrmann JM, Hamamoto S, Schekman R (2001). The ADP ribosylation factor-nucleotide exchange factors Gea1p and Gea2p have overlapping, but not redundant functions in retrograde transport from the Golgi to the endoplasmic reticulum. Mol Biol Cell 12, 1035–1045.
Stearns T, Kahn RA, Botstein D, Hoyt MA (1990). ADP ribosylation factor is an essential protein in Saccharomyces cerevisiae and is encoded by two genes. Mol Cell Biol 10, 6690–6699.
Stenmark H (2009). Rab GTPases as coordinators of vesicle traffic. Nat Rev Mol Cell Biol 10, 513–525.
Strom M, Vollmer P, Tan TJ, Gallwitz D (1993). A yeast GTPase-activating protein that interacts specifically with a member of the Ypt/Rab family. Nature 361, 736–739.
Suda Y, Kurokawa K, Hirata R, Nakano A (2013). Rab GAP cascade regulates dynamics of Ypt6 in the Golgi traffic. Proc Natl Acad Sci USA 110, 18976–18981.
Thomas LL, Fromme JC (2016). GTPase cross talk regulates TRAPPII activation of Rab11 homologues during vesicle biogenesis. J Cell Biol 215, 499–513.
Thomas LL, Joiner AMN, Fromme JC (2018). The TRAPPIII complex activates the GTPase Ypt1 (Rab1) in the secretory pathway. J Cell Biol 217, 283–298.
Thomas LL, van der Vegt SA, Fromme JC (2019). A steric gating mechanism dictates the substrate specificity of a Rab-GEF. Dev Cell 48, 100–114.e9.
Will E, Gallwitz D (2001). Biochemical characterization of Gyp6p, a Ypt/Rab-specific GTPase-activating protein from yeast. J Biol Chem 276, 12135–12139.
Xu P, Baldridge RD, Chi RJ, Burd CG, Graham TR (2013). Phosphatidylserine flipping enhances membrane curvature and negative charge required for vesicular transport. J Cell Biol 202, 875–886.
Yuan H, Davis S, Ferro-Novick S, Novick P (2017). Rewiring a Rab regulatory network reveals a possible inhibitory role for the vesicle tether, Uso1. Proc Natl Acad Sci USA 114, E8637–E8645.
Zerial M, McBride H (2001). Rab proteins as membrane organizers. Nat Rev Mol Cell Biol 2, 107–117.